CHAPTER I

INTRODUCTION

1.1 INTRODUCTION TO NANOTECHNOLOGY

Nanotechnology is an emerging technology which combines the features of physics, chemistry, biology, medicine and engineering. It has emerged in the last few decades of twentieth century that involves the development of new technologies for manipulating and simulating matter with dimensions smaller than 100 nm [1]. The word “nano” comes from the Greek word “nanos” which is the order of 10^{-9}m. The concept of nanotechnology was first given by Nobel Laureate Richard Feynman in 1959. The term nanotechnology was first given by Japanese scientist Norio Taniguichi of Tokyo Science University in 1974 [2].

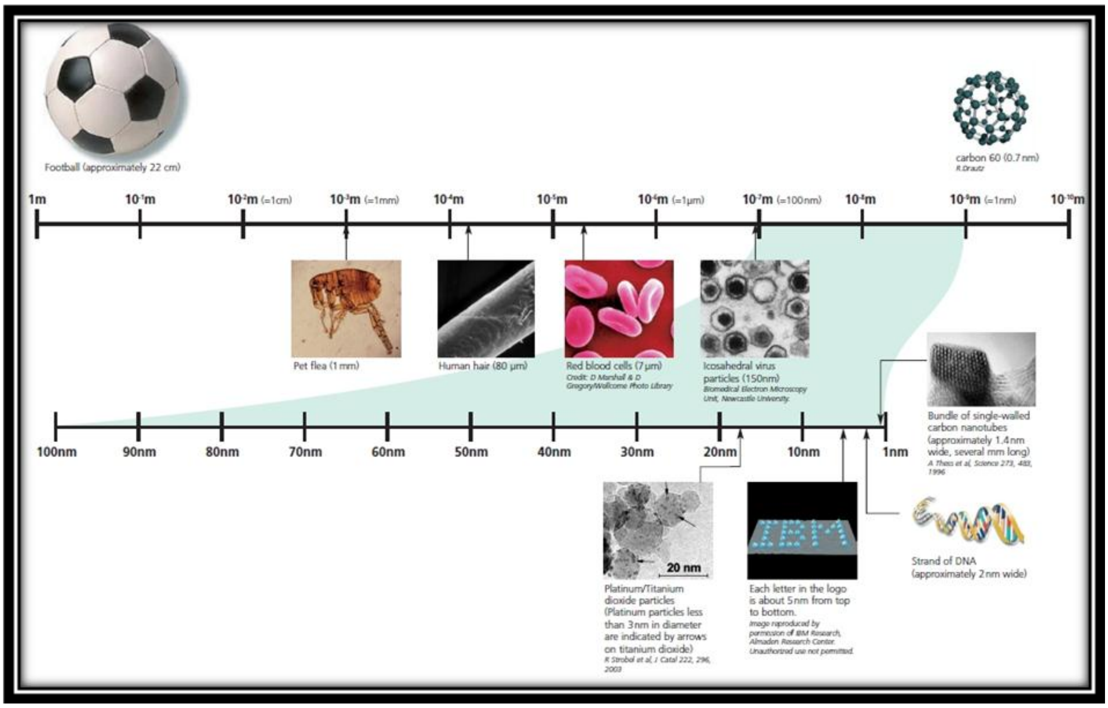

Figure 1.1 Nano scale and Nanostructures

The main impact of nanotechnology is to fabricate nanomaterials with advanced characteristics and functions materials at the atomic and molecular scales (1 and 100 nm) as shown in the Figure 1.1. It is an interdisciplinary technology which has gained more interest in many areas such as sensors, solar cells, resonators, drug deliver, mechanics, electronics, optics, biomedicine, plastics, energy electronics, aerospace etc., The important aspect of nanotechnology is that the properties such as chemical, electrical, magnetic, mechanical, optical, etc can be changed by controlling the size of materials. The enhanced properties like high surface area to volume ratio and quantum confinement are the major factors to produce new products. Thus the resultant nanostructure opens a new avenue in the field of science and technology. The integration of nanotechnology into larger systems has a profound impact on environment and society [3-4]. This initiates the interest among researchers towards a field of new physical phenomena and synthetic opportunities. The field of nanotechnology revolutionizes the ways of manufacturing the materials in industries which are found to cause commercial impacts on the society, economy and environment [5]**.**

1.2 NANOMATERIALS

Nanomaterials are the keystones of nanoscience and nanotechnology. In general, nanomaterials are defined as materials that are composed of particles in an agglomerated state with an average grain size less than 100 nanometers [6]. They are in the form of particles, tubes, rods or fibres. The composition of nanomaterials is similar to that of bulk but differ in their physio-chemical properties. The distinctive properties of nanomaterials such as optical, magnetic, electrical etc., at this scale has extraordinary impacts in wide range of applications like electronics, medicine etc., [7-8]

1.2.1. Classification of nanomaterials

The idea of classification of nanostructured materials was first given by Gleiter in 1995, and then it was further explained by Skorokhod in 2000. Nevertheless, the scheme devised by Gleiter and Skorokhod was not completely deliberated due to the zero-dimensional (0-D), one-dimensional (1-D), two 2 -dimensional (2-D) and three-dimensional (3-D) structures such as fullerene, nanotube and nanoflowers were to be classified based on this nomenclature. Therefore a modified classification scheme was reported by Pokropivny and Skorokhod for nanostructured materials in which 0-D, 1-D, 2-D and 3-D nanoscale components were incorporated [9-10]. Based on the Pokropivny scheme, the nanostructured materials can be classified as 0-D, 1-D, 2-D and 3-D depending on the materials that contain nanostructural elements in their dimensions. This dimensionality denotes the number of degrees of freedom in the particle momentum. The classification and examples of different forms of nanostructures are illustrated in the Figure 1.2

(a) 0D - Spheres and Clusters

(b) 1D - Nano-Fibers, Wires and Rods

(c) 2D - Films, plates and Networks

(d) 3D – Nanomaterial

Figure 1.2 Classifications of Nanomaterials

Zero-dimensional (0-D)

In 0-D system, the electrons are confined in their motion in all three directions and are measured within the nanoscale range. These include quantum dots and nanoparticles. Example: spheres and nanoclusters [11].

One-dimensional (1-D)

In 1-D system (quantum wire), the electrons are free to travel in one direction and confined in the other two directions and are measured outside the nanoscale. Example: Nanofibers, nanowires, nanorods, etc [12].

Two-dimensional (2-D)

In 2-D system (quantum wall), the electrons can easily move in two directions and are confined in one direction. Example: Nanofilms, nanoplates and branched structures [13].

Three-dimensional (3-D)

In 3-D system (bulk nanomaterials), the electrons are free to move in all three directions and there are no confinement and limitations. Example: powders, multilayer, fibrous and poly crystalline materials wherein nanostructural elements of 0-D, 1-D and 2-D are closely related with each other and form interfaces [14].

1.3. SYNTHESIS OF NANOPARTICLES

The nanoparticles are synthesized in a manner at which the resulting nanoparticles must have the following properties

- Identical in size,
- Identical in shape,
- Identical in chemical composition and crystal structure,
- Dispersed individually with any agglomeration.

Nanoparticles are generally synthesized by two different processes as shown in the Figure 1.3. In the top-down process, the rough particles lead to smaller particles by means of mechanical comminution. In bottom-up processes, the nanosized particles are formed by gas phase or liquid-phase reactions [15].

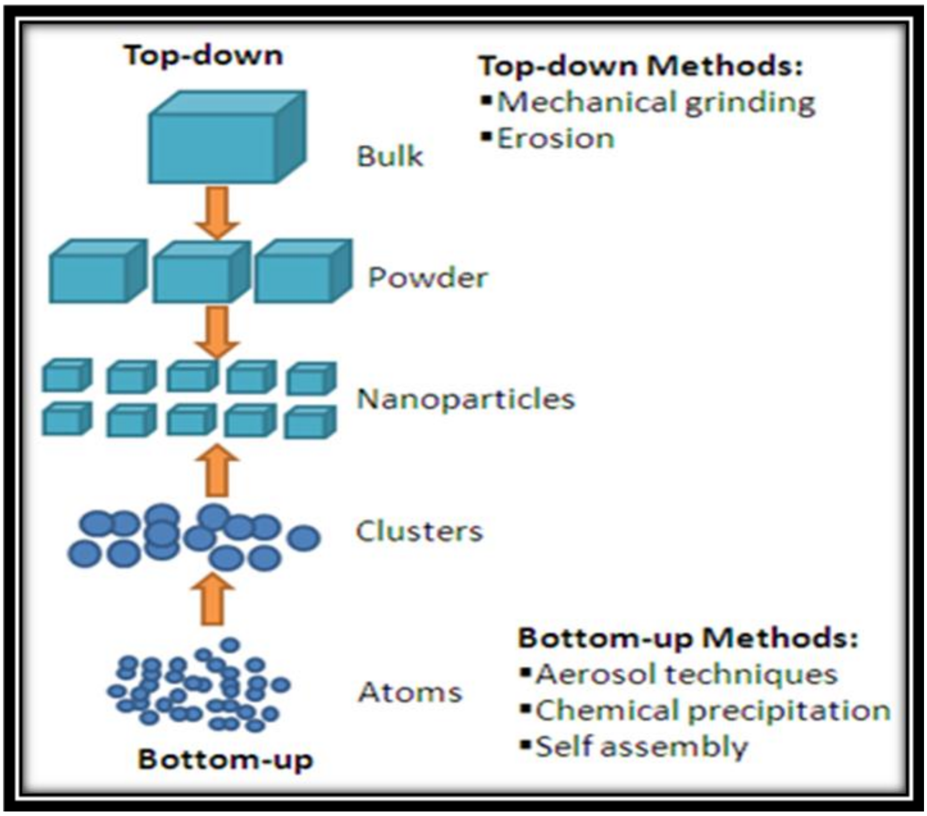

Figure 1.3 Top-down and bottom-up approach

1.3.1 Top-down approach

Top down approach is like sculpting a block from a stone. The desired shape is achieved by gradually eroding a piece of the base material. It is eroded first at the top of the blank piece and works the way down by removing the material from where it is not required. In nanotechnology, the top down approach are mainly divided into mechanical and chemical fabrication techniques [16]. Nanolithography is the most commonly used top down fabrication techniques. In this process, the required material is first protected by a mask and then the exposed material is etched away to get the desired structure. Etching of the base material can be done chemically using acids or mechanically using ultraviolet light, X-rays or electron beams, depending upon the resolution level required for features in the final product. This technique is also applied to the manufacture of computer chips [17-18].

1.3.2. Bottom-up approach

Bottom up fabrication is like building a brick house using more bricks. In nanotechnology bottom-up or self-assembly approaches uses chemical or physical forces for fabricating at the nano-scale range and to assemble the basic units into larger structures. Bottom up fabrication is done by placing atoms or molecules one at a time to build the desired nanostructure [19]. As component size decreases bottom-up approaches provide an increasingly important complement to top-down techniques. But is a time consuming processes. Thus self assembly techniques are employed where the atoms gets arranged by themselves as required. Quantum dots are manufactured by self-assembly technique. Quantum dots have rendered the top down approaches to semiconductor quantum dot fabrication, which is virtually obsolete. The inspiration for the bottom-up approach also comes from biological systems, where nature has harnessed chemical forces to create essentially all the structures needed by life. Researchers hope to replicate nature's ability to produce small clusters of specific atoms, which can then self-assemble into more-elaborate structures [20-21].

1.4 PROPERTIES OF NANOMATERIALS

The physical and chemical properties of the nanomaterials are closely dependent on their size and shape or morphology. Nanomaterials have the structural features in between atoms and the bulk materials. While most micro-structured materials have similar properties to the corresponding bulk materials but the properties of materials with nanometer dimensions are significantly different from those of atoms and bulks materials [22].

1.4.1 Structural properties

The increase in surface area and surface energy with decreasing particle size leads to changes in interatomic spacings. This is due to the internal pressure arising from the small radius of curvature in the nanoparticle induced by the compressive strain. In case of semiconductors and metals, the atomic spacings increase with decrease in the particle size. Metallic nanoparticles like gold and silver are known to have polyhedral shapes such as cuboctahedra, icosahedra, tetrahedran and decahedra. These nanoparticles may be regarded as multiply twinned crystalline particles (MTPs) in which the shapes can be understood in terms of the surface energies of various crystallographic planes [23-24].

1.4.2 Optical properties

The reduction of material dimension has strong effects on the optical properties. The size dependence is generally classified into two groups. One is due to surface plasmon resonance and the other is the increased energy level spacing as the system becomes more confined. The quantum size effect is very prominent for semiconductor nanoparticles, as the band gap energy increases with decrease in size of nanoparticles and the transition of the band gets shifted to higher frequencies. In such cases, the energy difference between the completely filled valence band and the empty conduction band increases gradually with decrease in size. [24] Quantum confinement produces a blue shift in the band gap as well as the appearance of discrete sub bands corresponds to quantization along the direction of confinement. The optical properties of nanostructured semiconductors are highly size dependent and thus can be modified by varying the size. Surface plasmon resonance is the excitation of all the free electrons within the conduction band which leads to an in phase oscillation. Surface plasmon resonance is generated if the size of a metal nanocrystal is smaller than the wavelength of incident radiation. For example, optical properties of gold and silver nanoparticles are size dependent. These nanoparticles change its colour with size due to surface plasmon resonance and hence they are widely utilized for molecular sensing, diagnostics and imaging [25-26].

1.4.3 Chemical properties

Nanoscale structures such as nanoparticles and nanolayers have high surface area to volume ratios that potentially differ in their crystallographic structures and that may lead to radical changes in their chemical reactivity. Nanoparticles often exhibit new chemistry as distinct from their larger particulate counterparts; for example, many new medicines will dissolve easily when it is in nanostructured form [27].

1.4.4 Mechanical properties

The mechanical properties of the nanomaterials such as hardness, elastic modulus, fracture, toughness, scratch resistance and fatigue strength etc are different from that of bulk materials which mainly depend on the size of nanoparticles. Enhancement of mechanical properties of nanomaterials is mainly due to the modification of these parameters that generally results from the structural perfection of the materials. The imperfections within the nano dimension migrate to the surface during the process of annealing and purifying of the material by leaving the perfect material structures inside the nanomaterials. The surfaces of nanomaterials tend to have less defects compared to that of bulk material which enhances the mechanical properties of nanomaterials [28-30].

1.4.5 Electronic properties

The changes that occur in electronic properties are mainly due to the influence of the wave property of the electrons. The size of the system is compared with the de Broglie wavelength of the electrons, since the discrete nature of the energy states becomes obvious eventhough the discrete energy spectrum is only observed in systems which are limited in all three dimensions. In certain cases, conducting materials become insulators below a critical length scale, since the energy bands get overlapped [31]. In macroscopic systems, electronic transport is determined primarily by scattering with phonons, impurities or other carriers or by scattering at rough interfaces. The path of each electron resembles a random walk and transport is said to be diffusive. In case of inelastic scattering, the system dimensions are smaller than the electron mean free path so that electrons can travel through the system without randomization of the phase of their wave functions. This increases the phenomena which are specifically related to the phase interference. If the system is sufficiently small so that all scattering centres can be eliminated completely and if the sample boundaries are smooth so that boundary reflections are purely specular, then electron transport becomes purely ballistic, with the sample acting as a wave guide for the electron wave function [32-33].

1.4.6 Thermal properties

The studies on thermal properties of nanomaterials have seen lower progressesion due to the difficulties of experimental measuring and controlling the thermal transport in nanoscale dimensions. In order to measure the thermal transport of nanostructures with high spatial resolution, Atomic force microscope (AFM) has been introduced with nanometer scale which provides a promising way to probe the thermal properties with nanostructures. The size, shape and large surface area changes the thermal properties of the nanomaterials which exposes a small different behaviour when compared to the bulk. For example, because of the tubular structures of carbon nanotubes, they have extremely high thermal conductivity in axial directions, leaving high anisotropy in the heat transport in the materials. The interfaces are also a very important factor for determining the thermal properties of nanomaterials [34-35]

1.4.7 Magnetic properties

Magnetic nanoparticles are used in a various range of applications such as ferrofluids, colour imaging, bio processing and refrigeration as well as high storage density magnetic memory media. The consequence of large surface area to volume ratio leads to differing magnetic properties by magnetic coupling of atoms with neighbouring atoms. Since the surface energy provides sufficient energy for domains to switch polarization directions spontaneously, hence the ferromagnetic particles become unstable when the particle size reduces below a certain size. As a result, the ferromagnetic become paramagnetic. However, the paramagnetic behaves differently from the conventional paramagnetic and is referred to as super paramagnetic. The bulk ferromagnetic materials usually form multiple magnetic domains, hence the small magnetic nanoparticles often consist of only one domain and exhibit a phenomenon known as super paramagnetism. In this case the overall magnetic coercivity reduces the magnetic polarization of various particles and is randomly distributed due to thermal fluctuations and only become aligned in the presence of an applied magnetic field [36-37].

1.5 APPLICATIONS OF NANOTECHNOLOGY

Nanotechnology has wide range of applications in the field of electronics, fuel cells, batteries, agriculture, food industry, cosmetics, paints, textiles, biomedicial etc... as shown in the Figure 1.4 [38].

Figure 1.4 Applications of Nanotechnology

1.5.1 Nanoclays

Clays have naturally occurring nanoparticles that have been used for long time as construction materials and are undergoing continuous improvement. Nanoclays based comsposites and nano-sized flakes of clay are also applied in car bumpers [39].

1.5.2 Nanocoatings and nanostructured surfaces

In case of self-cleaning, window coatings are done by controlling the thickness of material at the nano or atomic scale, which is coated using activated titanium dioxide. These nanocoatings are designed to be highly hydrophobic (water repellent) and antibacterial. Coatings based on nanoparticle oxides catalytically that destroy chemical agents. Nanoscale multilayers or intermediate layers are used for wear and scratch-resistant hard coatings [40].

1.5.3 Drug Delivery

In recent years, polymer matrix encapsulated nanocapsusles and nanospheres are used for drug delivery at which the drugs can be dispersed into the matrix. The advantage of using nanocapsules is that they target only particular organs as carriers of DNA in gene therapy. They have the ability to deliver proteins, particles and genes and can circulate for long period of time [41-42].

1.5.4 Energy storage

The utilization of nanotechnologies in electrical energy stores like batteries and super-capacitors are one of the outstanding applications of nanotechnology. Lithium-ion technology is regarded as the most promising electrical energy storage devices due to its high cell voltage and the excellent energy and power density. The capacity and safety of lithium-ion batteries can be enhanced by using new ceramic, heat-resistant and flexible separators and high-performance electrode materials. Carbon nanotubes have applications in battery technology. Lithium has a charge carrier in some batteries and can be stored inside nanotubes. One lithium atom can be stored for every six carbons of the tube. Storing hydrogen in nanotubes is another possible application: one that is related to the development of fuel cells as sources of electrical energy for future automobiles. For example, the Evonik Company commercializes systems such as hybrid and electric vehicles as well as stationary energy storage devices. Another important field in energy storage is thermal energy storage. Nanoporous materials like zeolites which are adsorption based storage material are applied as heat storage in distinct heating grinds, industries, etc., [43- 45]

1.6. REVIEW OF LITERATURE

Changjing Fu et. al., [46] have prepared high quality reduced graphene oxide (rGO) nanosheets from natural graphite through oxidation by solvothermal reduction method. The morphology, structure and composition of GO and rGO nanosheets were characterized by X-ray diffraction (XRD), scanning electron microscope (SEM), transmission electron microscope (TEM), Raman spectrum, and X-ray photoelectron spectroscopy (XPS). The electrochemical performances of rGO nanosheets for lithium-ion batteries were evaluated using coin-type cells versus metallic lithium. Thus the obtained rGO exhibited a higher reversible specific capacity of 561 mAh g^{-1} at a current density of 100 mA g^{-1} and 166 mAh g^{-1} at a current density of 4000 mA g^{-1}.

The Synthesis of Graphene oxide from a natural graphite powder by modified Hummers method were reported by **Indranil Roy et.al.,** [47] They have demonstrated the electrochemical characterization of RGO/Ag nanocomposites which have been synthesized via green approach and characterized by XRD, FTIR, UV-vis spectroscopy, TEM and EDAX. The electro-chemical behaviour indicates that GO has the lowest current and it continuously increases for RGO and RGO/Ag nanocomposites.

N.I. Zaaba et.al., [48] have studied the influence of different solvents on the structure and electrical properties of graphene oxide. They have synthesized GO by using Modified Hummers method from graphite flakes. In this method, they have synthesized GO without sodium nitrate ($NaNO_3$) and also carried out the reaction at room temperature. The prepared GO powders were then dissolved into different solvents like acetone and ethanol. The dissolved GO was spin-coated onto silicon wafer and IDE to produce acetone-GO (A-GO) and ethanol-GO (E-GO). The current voltage pattern indicated that due to large agglomeration and contact between the flakes the E-GO produces higher current flow than A-GO. FTIR showed that both A-GO and E-GO contains several functional groups such as hydroxyl, epoxy, carboxyl and carbonyl groups. XRD showed that due to the lower diffraction peak of A-GO, the interlayer spacing of A-GO sample was slightly higher than E-GO sample.

M. Nur Hossain et al., [49] have reporedt a unique nanocomposite consisting of Cu nanoparticles (NPs) and reduced graphene oxide (rGO) supported on a Cu substrate with a high catalytic activity for CO2 reduction. The nanocomposite was optimized in terms of the composition of Cu NPs and rGO as well as the overall amount. A gas chromatograph was employed to analyze the gaseous products, whereas a chemical oxygen demand (COD) method was proposed and utilized to quantify the overall liquid products. The optimized nanocomposite could be effectively reduce CO2 to CO, HCOOH and CH4 with a Faradaic efficiency (FE) of 76.6% at −0.4 V (vs. RHE) in a CO2 saturated NaHCO3 solution. The remarkable catalytic activity, high FE, and excellent stability make this Cu-rGO nanocomposite promising for the electrochemical reduction of CO2 to value-added products to address the pressing environmental and energy challenges.

Z. Hu et al., [50] have summarized the research works of graphene-reinforced metal matrix composites. Graphene has been thought to be an ideal reinforcement material for composites due to its unique twodimensional structure and outstanding physical and mechanical properties. It is expected to yield structural materials with high specific strength or functional materials with exciting thermal and electrical characteristics. This review have introduce all kinds of graphene-reinforced metal matrix composites that have been used widely

Jonghoon Choi et.al., [51] have prepared graphene supported CuO nanocomposites by controlling the condition of a copper-precursor on graphene oxide (GO) by subsequent thermal treatments. The morphological and chemical structures of the nanocomposites were systemically evaluated by XRD, XPS and TEM. The rGO based CuO nanocomposites exhibited a much higher catalytic activity than bare CuO NPs toward the decomposition reaction of dye molecules under visible light illumination.

Zhimin Luo et.al., [52**]** have synthesized reduced graphene oxide/chitosan oligosaccharide using chemical reduction of graphene oxide. The potential measurement indicated that RGO-CTSO were highly stable in acidic aqueous solution. The direct electron transfer of E. coli on the RGO-CTSO-modified GCE was studied by cyclic voltammetry. The results showed that compared with GCE and RGO-modified GCE, the RGO-CTSO modified GCE enhanced the direct electron transfer which was more suitable for the adhesion growth of E. coli. The biocompatibility and versatility of RGO-CTSO might be used as a promising anode material in microbial fuel cells.

Zhihong Zhang et.al., [53] have prepared a DNA-modified nanocomposites by 3D reduced graphene oxide and chitosan nanoparticles using one-step method and tested for the detection of mercury in drinking water. The prepared electrochemical biosensor provided goodsensitivity toward the determination of Hg^{2+} with a low detection limit of 0.016 nM, ranging from 0.1 nM to 10 nM. Hence, this proposed CS@3D-rGO@DNA-based electrochemical strategy is feasible and may offer a sensitive, selective, simple and cost-effective method for Hg^{2+}.

Dooa Arif et. al., [54] have synthesized antibacterial cotton fabric using chitosan-silver nanoparticles. Scanning electron micrograph (SEM) attributed that the presence of CS-AgNPs was formed on the surface of cotton fabric. The bacterial efficiency of the synthesized nanoparticles was tested gainst two gram negative bacteria (Escherichia coli, Pseudomonas aeruginosa) and two gram positive bacteria (Bacillus cereus, Staphylococcus aureus)

S. Archana et.al., [55] have synthesized Graphene oxide Zinc oxide (GO-ZnO) nanocomposite by a simple hydrothermal method. SEM and TEM analysis showed that the ZnO nanoparticles were distributed and closely anchored on the graphene oxide layers. The nanocomposite showed an extraordinary adsorption capacity and the fast adsorption rates for the removal of methylene blue (MB) and methyl orange (MO) from an aqueous solution. They also have investigated the adsorption isotherm, kinetics and thermodynamics in detail and the results showed that the adsorption data was best fitted to Langmuir adsorption isotherm model. The calculated monolayer adsorption capacity is 265.95 and 714.28 mg/g for MB and MO, respectively. Adsorption kinetics follows the pseudo-second-order kinetic equation. Thus, the prepared nanocomposite can be effectively utilized for the removal of organic dyes. These results suggest that the antimicrobial activities are caused by the membrane stress. The direct contact with sharp edges causes the membrane stress on cells, thereby resulting in the rupture. The physicochemical applications of graphene-based materials are specifically targeted to reduce the risks in environment.

S. Gayathri et. al., [56] have synthesized Zinc oxide/Graphene (GZ) nanocomposites with different concentrations of ZnO through simple chemical precipitation method. The ZnO nanoparticles decorated graphene sheets were clearly visible in the field emission scanning electron micrograph and the energy dispersive X-ray spectrometry analysis showed the purity of the prepared samples. Raman mapping was employed to analyze the homogeneity of the prepared samples. The diffuse-reflectance spectra showed the absorption in the visible region which clearly indicated the formation of GZ nanocomposites. The photocatalytic activity of ZnO confirmed that the GZ composites exhibited a higher photocatalytic activity than pristine ZnO which can be applied in photocatalysis.

Antonella Arena et al., [57] have synthesized chitosan:CuOx nanocomposite by electrodeposition method and was characterized by means of spectrophotometry, frequency domain electrical measurements and morphological analysis. Solid state electrochemical cells having pure chitosan as the electrolyte and using chitosan:CuOx as the electrode, are developed and characterized by means of electrical measurements performed in the +1 V voltage window. The current-voltage loops of the cells, measured in deionized water, are found to reversibly change in response to hydrogen peroxide added to the water in 0.2 M subsequent steps. This clearly distinguishes from changes recorded in response to other analytes, can be exploited in order to develop a hydrogen peroxide sensor able to work without the need for any supporting electrolyte.

Sangiliyandi Gurunathan et. al., [58] have demonstrated a simple, environmentally friendly, and dependable approach for the synthesis of rGO–Ag nanocomposites using the natural enzyme TAPE. The synthesized nanocomposites were characterized using UV-Vis, FT-IR, Raman spectroscopy, XRD, SEM, and TEM techniques. These results showed that AgNPs with diameters of approximately 20 nm are uniformly deposited on the surface of rGO. Moreover, the rGO–Ag nanocomposite showed excellent solubility and stability for more than 3 months.

The as synthesized nanocomposite displayed significant cytotoxicity and showed high effective apoptotic activity against ovarian cancer cell.

Sandhya P K et.al., [59] have reported the synthesis of two forms of graphene derivatives namely, reduced graphene oxide (RGO) through reduction using potato starch and zinc oxide decorated RGO (ZnO-RGO). The characterization was done by FT-IR, XRD, Raman spectra and TEM techniques. The antibacterial activity was studied by well diffusion method. Their results showed that ZnO-RGO is more efficient than that of RGO in their antibacterial properties which they attributed the synergistic effect of ZnO and RGO towards the bacteria in the nanocomposite. Moreover they have find that the antibacterial effect of ZnO-RGO towards. Considering the fact that graphene-based materials are less toxic towards mammalian cells, both RGO and ZnO-RGO have developed could find applications in the field of medicine and life sciences.

Yan-Wen Wang et. al., [60] have prepared ZnO/ GO nanocomposites by a facile one-pot reaction to achieve superior antibacterial properties without damaging other species. The prepared ZnO nanoparticles with a size of about 4 nm were homogeneously anchored onto GO sheets. They tested the antibacterial activity and cytotoxicity of the ZnO/GO composites by Escherichia coli and Cervica cancer cell line (HeLa) respectively. GO helped the dispersion of ZnO NPs, slowed the dissolution of ZnO that acted as the storage site for the dissolved zinc ions, and enabled close contact of E. coli with ZnO nanoparticles. The results indicate that the ZnO/GO composites are promising disinfection materials to be used in surface coatings on various substrates to effectively inhibit bacterial growth, propagation, and survival in medical devices.

Chandrama Sarkar et. al., [61] have developed copper oxide– reduced graphene oxide (CuO–rGO) nanocomposites by a facile and novel hydrothermal method In this method the simultaneous formation of CuO and reduction of GO takes place without using any foreign materials. The synthesized composites were characterized by FTIR, XRD, SEM and EDAX spectroscopy. The nanocomposites possessed excellent catalytic activity towards reduction of 4-NP to 4- aminophenol

(4-AP). The reaction kinetics followed a pseudo-first-order rate law and the maximum value of the rate constant is 13.951 min^{-1}, which was superior to all other reported works. The catalyst could be easily regenerated and reused with good recyclability even for up to five catalytic cycles.

Dipanwita Majumdar et. al., [62] have fabricated the reduced graphene oxide-Copper(II)oxide (rGO-CuO) nanocomposite by sonochemical technique. The optimum amounts of CuO and functionalized-graphene phases established strong superior electrochemical mark. The spectroscopic, microscopic, surface and thermal analyses of the synthesized nanocomposites revealed that the nanocompositesis of stable, nanostructure morphology with large surface area which opened the scope for its supercapacitive applications. The electrochemical performances were investigated by cyclic voltammetry and chronopotentiometric charging/discharging cycles at a current density of $1Ag^{-1}$ in the potential window of -0.3V to + 0.8V in 0.5 M Na_2SO_4 aqueous medium. The result showed that the rGO-CuO nanocomposite displayed appreciable specific capacitance (Cs= 227 Fg−1) compared to the reduced graphene oxide (rGO) (136.4 Fg^{-1}) and bare copper oxide (30.1 Fg^{-1}).

Ajay Gupta et.al., [63] have synthesized new hybrid molecules containing flavanone with triazole by merging the Michael addition. They have synthesized copper oxide/reduced graphene oxide nanocomposite by one pot synthesis. The catalyst could easily be recycled and reused in seven consecutive runs without compromising the product yields.

J.Vinoth Kumar et.al., [64] have developed the electrochemical sensor for trace level detection of 4-aminophenol (4-AP) in environment. The MoS_2 nanoclusters were fabricated by simple hydrothermal treatment without using any other organic templates or surfactants. The formation of MoS_2 nanoclusters were characterized by XRD, FT-IR, Raman, EDAX, SEM and SAED analysis. The results attributed that the MoS_2 modified GCE (MoS2/GCE) showed good electrocatalytic activity towards the redox reaction of 4-AP by means of cyclic voltammetry and differential pulse voltammetry. The detection of 4-AP using DPV delivered excellent sensitivity with low detection limit of 0.03 (± 0.008) μM and good linearity in the range of 0.04-17 μM for MoS_2/GCE. The sensitivity for the developed electrode is 4.278 (± 0.058) μA mM^{-1} cm^{-2}. Thus the developed sensor displayed good repeatability, reproducibility and selectivity.

Manish Kumar et. al., [65**]** have synthesized graphene oxide/silver (GO/Ag) nanocomposites by chemical reduction method with EG/$NaBH_4$ as a solvent and the reducing agent. The GO/Ag nanocomposites were characterized by XRD, TEM and RAMAN. The highly monodispersed stable crystalline silver nanoparticles having a face-centered cubic (fcc) phase were confirmed by X-ray powder diffraction (XRD) from GO. SEM and TEM images showed that the Ag nanoparticles with an average size of 18 nm were dispersed on the GO sheet with a narrow size distribution. The intensities of the Raman signal of GO/Ag nanocomposites were gradually increased with attachment of Ag nanoparticles. Electrochemical investigations indicates that the nanocomposites possessed an excellent performance towards the detection of 4-nitrophenol. They also have demonstrated the reduction of 4-nitrophenol to 4-aminophenol by $NaBH_4$. Hence, the prepared nanocomposites exhibited high activity and stability for the catalytic reduction of 4-nitrophenol.

Tamas Nemeth et. al., [66] have developed a micellar electrokinetic chromatographic (MEKC) method for the quality control of paracetamol. The influence of several factors (surfactant concentration, buffer concentration, pH and applied voltage were studied during the development and optimization. Phosphate buffer (pH 9.0) containing sodium dodecyl sulphate (75mM) and the applied voltage of about 25 kV was found to be ideal parameters and the analysis time was 10 min. The limit of quantitation for 4-aminophenol were 6µgml^{-1}, the linearity were studied in the concentration ranges from 20 to 260µgml^{-1} for paracetamol and 20–150µgml^{-1} for 4-aminophenol.

Graziella Scandurra et. al., [67] have prepared a conducting composite by dispersing multi-walled carbon nanotubes (MWCNTs) into a host matrix consisting of Nafion and was electrochemically doped with copper. The nanocomposite was characterized and used to modify one of the gold electrodes of simply designed electrochemical cells having copier grade transparency sheets as substrates. The intensity of redox peak current of p-AP was linearly proportional to the concentration of p-AP with the range from 0.2 to 1.6 μM, and detection limit of 90 nM and sensitivity of 7 μA (μM^{-1}) cm^{-2}. The results showed that Au/Nafion/Au-MWCNTs–Nafion:Cu cells could be successfully used in order to detect the presence of (PAP) in water, without the need of any supporting electrolyte.

Priya Arulselvi Ramasubramanian et. al., [68] have synthesized a novel two-dimensional MoS_2 microspheres by a facile hydrothermal method and the phase, structural and functional groups are characterized using XRD, SEM, FT-IR and Raman spectroscopy analysis. They modified the MoS_2 microspheres on glassy carbon electrode (GCE) for the detection of 4-aminophenol (4-AP). The MoS_2 modified GCE showed high electrocatalytic activity towards oxidation of 4-AP in a phosphate buffer solution (pH7.0). Under optimized conditions, the electrocatalytic activity of 4-AP exhibited the strong redox peak over a wide range from 2 to 8 nM with detection limit of about 2 nM. Hence, the MoS_2 sensor could be used for real time 4-AP detection in waste-water.

Leandro Yoshio Shiroma et. al., [69] have constructed a sensitive microfluidic paper-based device for the electrochemical detection of paracetamol and 4-AP. A baseline separation level of the analytes could be obtained in 0.1 mol L^{-1} acetate buffer solution at pH 4.5 and by injecting 500 nL of the standard solutions at 12 mm from the working electrode. The electrochemical detection system was created at the end of the channels through a process known as sputtering. The previously separated analytes were detected at the end of the hydrophilic separation channel by applying a potential of 400 mV vs. pseudo Au on the working electrode.

Huanshun Yin et.al., [70] have fabricated graphene–chitosan composite film modified glassy carbon electrode (GCE) to determine 4-aminophenol (4-AP). The experimental conditions were optimized and the kinetic parameters and the oxidation mechanism were discussed. The oxidation peak current is directly proportional to the concentration of 4-AP with the detection limit was 0.057μM (S/N = 3). They also have determined 4-AP determined in water samples and paracetamol tablets.

A.T.Ezhil Vilian et. al., [71] have prepared a electrochemical sensor for the detection of 4-aminophenol (4-AP) by the electrodeposition of poly-L-glutathione on the surface of reduced graphene oxide (RGO) to form a composite matrix on a glassy carbon electrode. The morphology and structure of RGO/P-L-GSH modified GCE were characterized by scanning electron microscopy (SEM), FT-IR spectroscopy and electrochemical impedance spectroscopy. As an electrochemical sensor, the RGO/P-L-GSH modified GCE composite exhibited strong catalytic activity toward the oxidation of 4-AP by cyclic voltammetry (CV) and chronoamperometry. The electrochemical sensor demonstrated good anti-interference ability in the presence of glucose, fructose, paracetamol, ethanol, l-isoluecine, l-histidine, lcysteine, dopamine, l-serine, l-tyrosine, phenylalanine, urea, hydrogen peroxide, K^+, Ca^{2+}, Na^+, F^-, SO_4^{2-}, Cu^{2+}, Fe^{3+}, Zn^{2+}, folic acid and ascorbic acid.

Anna Regiel-Futyra et. al., [72] have described the synthesis and characterization of non-cytotoxic nanocomposites either colloidal or as films exhibiting high antibacterial activity. For the synthesis of gold nanoparticles (AuNPs), the biocompatible and biodegradable natural bio polymer chitosan (CS) was used as reducing and stabilizing agent. They have used three different chitosan grades varying in the average molecular weight and deacetylation degree (DD) with an optimized gold precursor concentration. Several factors were analyzed in order to study the antimicrobial and cytotoxicity. In contrary the nanocomposites showed less cytotoxicity against mammalian somatic and tumoral cells. They produced a disruptive effect on the bacteria wall while their internalization was hindered on the eukaryotic cells. This selectivity and safety made them potential candidate for antimicrobial coatings in the biomedical field.

S. Govindan et. al., [73] have synthesized Ag and chitosan–silver (CS–Ag) nanocomposite materials by a simple chemical method. The CS–Ag nanocomposites were characterized using FESEM, XRD and FTIR. The XRD pattern indicates that the formed silver is of cubic structure. The spherical morphology of silver nanoparticles is confirmed from the FESEM image. FTIR spectroscopy was used for the structural elucidation. CS–Ag nanocomposite exhibited good antimicrobial and antitumor properties.

Richard Justin et. al., [74] have synthesized chitosan–reduced graphene oxide (rGO) nanocomposites through a biocompatible reduction process and they were the first to report the applications in transdermal drug delivery devices like microneedle arrays. They improved the mechanical properties of chitosan by the addition of rGO. The different concentrations of rGO (1 wt% and 2 wt%) was chosen to undergo drug delivery testing. The result attributed that the addition of rGO increased the electrical conductivity of chitosan, allowing the nanocomposites to be used for drug delivery applications. The concentration of rGO was proven to be an important factor for drug delivery due to the bonding of drug onto the rGO thus for higher concentration more substantial drug was released with a controlled drug release rate. The nanocomposites also exhibited pH dependent release behaviour, with a reduced release rate in the presence of an acidic medium.

Dasan Mary Jaya Seema et.al., [75] have prepared a anticancer nanocomposites based on graphene oxide (GO) as an anticancer agent. The prepared nanocomposites were characterized using XRD, Raman, UV-Vis, FT-IR, DLS and TEM etc. These results suggests that GO on binding with PEITC could be developed as an efficient drug carrier for pharmaceutical applications in cancer chemotherapies.

1.7 MATERIALS

1.7.1 Carbon nanostructures

Carbon is one of the most abundant elements on the Earth that plays a critical role in the bio and ecosystems. The term carbon is derived from the Latin word ‘carbo’ meaning charcoal which forms stable allotropes [76]. Carbon with sp^3 hybridization gives rise to diamond like carbon and sp^2 hybridization leads to the formation of graphitc carbon**.** Many other allotropes of carbon such as buckminsterfullerene (C60), carbon nanotubes (CNTs) and graphene have been discovered during the last 30 years as shown in the Figure 1.5 [77-78]. Each of the allotrope has its own importance and applications. Both diamond and graphite possess excellent mechanical properties, optical properties and thermal conductivity due to the small size, close packing of carbon atoms, as well as short and strong chemical bonds between these atoms. Fullerenes also known as bucky balls are discovered in 1985. Fullerenes are spherical in shape containing pentagonal rings that prevent the sheet from being planar. They can be applied in solar cells, fuel cells, sensors etc [79-80].

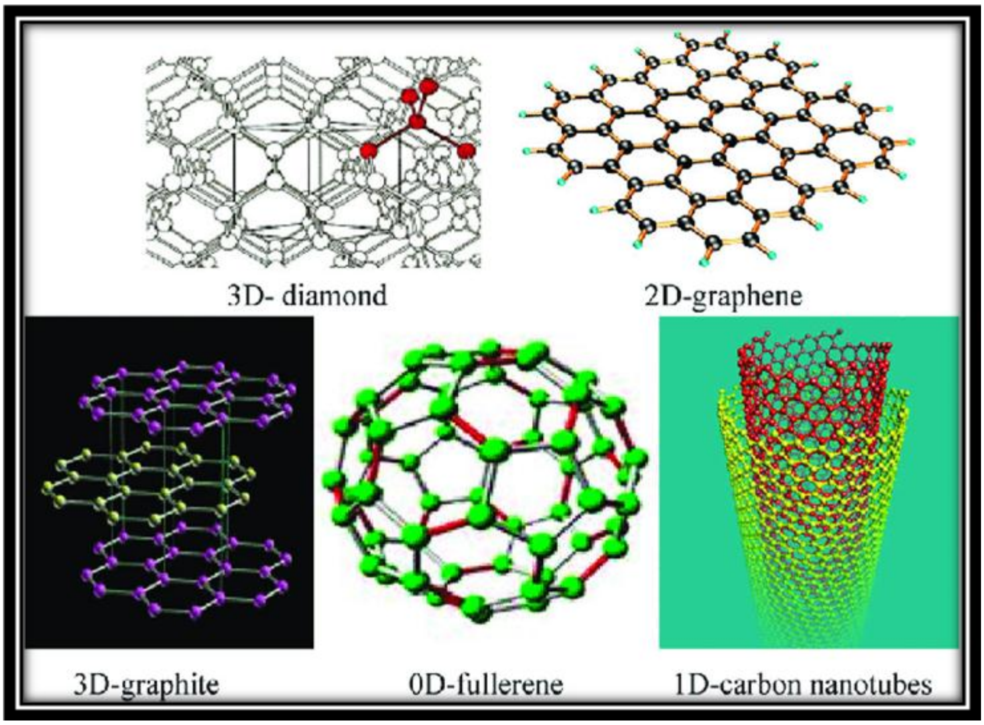

Figure 1.5 Different structural forms of Carbon: Diamond, Graphene, Graphite, Fullerenes and Carbon nanotubes

Fullerenes can be considered as wrapped graphene obtained with the introduction of positive curvature defects (pentagons) in graphene. CNTs are cylindrical nanostructure having high length to diameter ratio [81-82]. CNTs are discovered by Sumio Iijima in1991 and one dimensional CNTs are obtained by rolling graphene in one direction and reconnecting the bonds. CNTs have been used in chemical and biological sensors, drug delivery, genetic engineering, fuel cells etc.

CNTs and graphene possess outstanding properties such as high tensile strengths, ultra-lightweight, excellent thermal and chemical stability, high surface area and favourable electronic properties. Carbon materials have fascinated interest in the development of alternative clean and sustainable energy technologies. For example, p-type semiconducting polymers with fullerence are considered as an important material in organic photovoltaics [83-85].

1.7.2 Graphene

Graphene is the youngest of all the material which was first coined the term by Hanns–Peter Boehm in 1962 as a combination of graphite and the suffix –ene. It is the strongest and thinnest material of the universe with an excellent conductor of both heat and electricity [86]. The thickness of a graphene layer is about 0.33 nm which act as building block for other allotropes of carbon such as graphite, diamond, fullerene and carbon nanotubes (CNTs). Graphite and diamond are two well known allotropes of carbon, while fullerene and CNTs are newly discovered forms. In 1947, Wallace stated that in order to study graphite, first the study of single sheet of graphite is necessary [87]. In 2004, the existence of 2D crystals became true when A. Geim and K. Novoselov successfully exfoliated single sheet of graphite called graphene by scotch tape mechanical exfoliation method. They found carbon to carbon bond length in graphene is small but strong, which prevent thermal fluctuations in it and stabilize it. They have been awarded the Nobel Prize in Physics (2010) by Royal Swedish Academy of Sciences for experiments on graphene from physical point of view, these are zero dimension structures having discrete energy levels [88-89].

Graphene, a single layer of carbon atoms arranged in a honeycomb lattice bonded by sp^2 hybridization. It consists of two equivalent sub-lattices of carbon atoms bonded with σ bond, which is a basic building block for all other graphitic materials of various dimensionalities [90-92]. The remarkable electrical, physical, thermal, optical and mechanical properties of graphene makes it a super material for replacing carbon fibers in composite materials to make lighter aircraft and satellites, replacing silicon in transistors, supercapacitors, sensors for detection of hazardous chemicals, photovoltaic applications, optoelectronics, embedding the material in plastics to enable them to conduct electricity, stiffer–stronger–lighter plastics, leak–tight, plastic containers that keeps food fresh for weeks [93].

1.7.3 Structure of Graphene

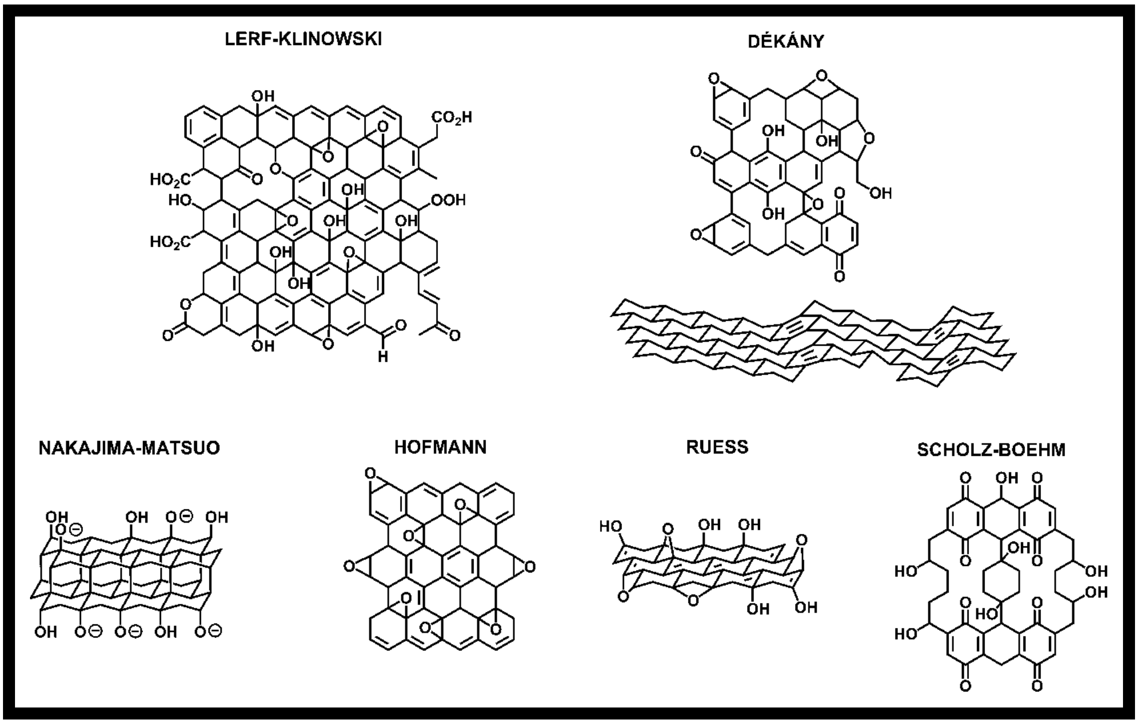

Figure 1.6 Structure of Graphene

The structure of GO is still unique due to its nonstoichiometry and it can be varied depending on the oxidation conditions. The nature of oxygen-containing groups and their arrangements across the carbon network are critical for obtaining an accurate structure of GO. Microscopic techniques can provide deep insights into the types of oxygenated functional groups in GO and their distributions [94]. Several models have been proposed so far such as the Hofmann, Ruess, Scholz–Boehm, Nakajima–Matsuo, Lerf–Klinowski and Dekany’s models. Hofmann and Holst presented the very first structure of graphite based on sp^2 hybridised system. This structure consists of repeating units of 1,2-epoxides randomly distributed across the basal-planes of graphene [95]. However in 1946, Ruess proposed a new structure based on sp^3 hybridised basal-planes which is in contrary to Hofmann and Holst model. This structure consists of 1,3-epoxide and hydroxyl groups due to the presence of hydrogen atoms found in graphite oxide. Later in 1969, Scholz and Boehm proposed a model which is made up of only hydroxyl and ketone groups. The subsequent model introduced by Nakajima and Matsuo gave rise to a structure which is very similar to a graphite intercalation compound. This structure differed from the above ones in which the oxygen atoms in epoxies link the adjacent layers. Szabo and Dekeny's model incorporated the features of both Sholz–Boehm and Ruess' models. The most widely used model is the Lerf–Klinowski. They have developed their model based on the experimental results obtained by solid NMR and different XRD analysis [96-97]. It is nonstoichiometry at which the epoxy (1,2-ether) and hydroxyl are the major functional groups that are randomly decorated across the carbon groups. Dékány and coworkers proposed a nonplanar structure by extending Ruess and Scholz-Boehm models based on elemental analysis, XPS, diffuse reflectance infrared Fourier transform spectroscopy, electron spin resonance, TEM, XRD and NMR. This model is composed of two distinct domains consists of trans linked cyclohexane chairs and corrugated hexagon ribbons. Thus the cyclohexane chairs consists of 1,3-epoxide and tertiary hydroxyl groups and the hexagon ribbons are occupied with cyclic ketones and quinines [98-100].

1.7.4 Properties of graphene

Graphene has many unique properties such as optical, electrical, mechanical and thermal properties which make it an ideal material in various fields like solar cells, drug delivery, sensors, batteries etc., [101].

1.7.4.1 Electronic properties

One of the most important properties of graphene is its charge carriers which behave as a massless relativistic particles or the Dirac fermions. It is known that graphene is a zero-gap 2D semimetal with high electrical conductivity. The electrons and holes which are known as charge carriers overlap between the valence band and the conduction band that scatters under ambient conditions. The electronic properties of graphene can be studied fundamentally by the bonding and anti-bonding of the pi orbitals [102].

1.7.4.2 Optical properties

Graphene is a thin sheet and the single sheet of graphene can absorb only 2.3% with a negligible reflectance of about 0.1 %. Adding another layer of graphene increases the absorbance by approximately the same value (2.3%). Thus the absorbance increases linearly with the layer numbering from 1 to 5. This linearity are in consistence with the theoretical results obtained with a model of non-interacting massless Dirac fermions. The transparency of graphene depends on the fine structure constant which describes the coupling between the light and relativistic electrons. Graphene can be used effectively in solar cells by combining the amazing features of optical and electrical properties [103].

1.7.4.3 Thermal properties

Graphene has unique thermal properties due to its strong, anisotropic bonding and low mass of the carbon atoms. The study of thermal conductivity of graphene has important implications in graphene–based electronic devices. The thermal conductivity of single-layer suspended graphene measured at room temperature depending on the size of graphene sheet is 3000-5000 $Wm^{-1}K^{-1}$. Thus below the room temperature, the specific heat of graphene is higher than that of graphite and diamond. Moreover, due to the continued progress in the electronic industries, results in the reduction of device size and as a result of this, the circuit density increases. Hence the heat removal has become a crucial issue for proper functioning of the device. Thus the material with high thermal conductivity is required for dissipating the heat from electronic devices. This indicates that graphene based composites have interesting prospect for heat sinking applications due to their ultra–high thermal conductivity [104].

1.7.4.4 Mechanical properties

Mechanical strength is one of the important properties of graphene which can make it a superior material compared to the other known materials. The stiffness, roughness and strength are the extraordinary fundamental mechanic properties of graphene. The important factors for high mechanical strength are small C–C bond length (0.142 nm) and defects free–surface. The elastic modulus and the intrinsic strength measured for defect free monolayer graphene sheet are 1.0 TPa and 130 GPa suggesting the strongest material measured ever. Theoretical work has been carried out to investigate the mechanical properties of zigzag graphene and armchair graphene nano ribbons, indicated that the critical mechanical loads and buckling of armchair ribbons are smaller than those for zigzag ribbons. In addition, external mechanical loads can change the electronic properties of graphene, such as field emission performance [105-106].

1.7.5 Reduced Graphene Oxide

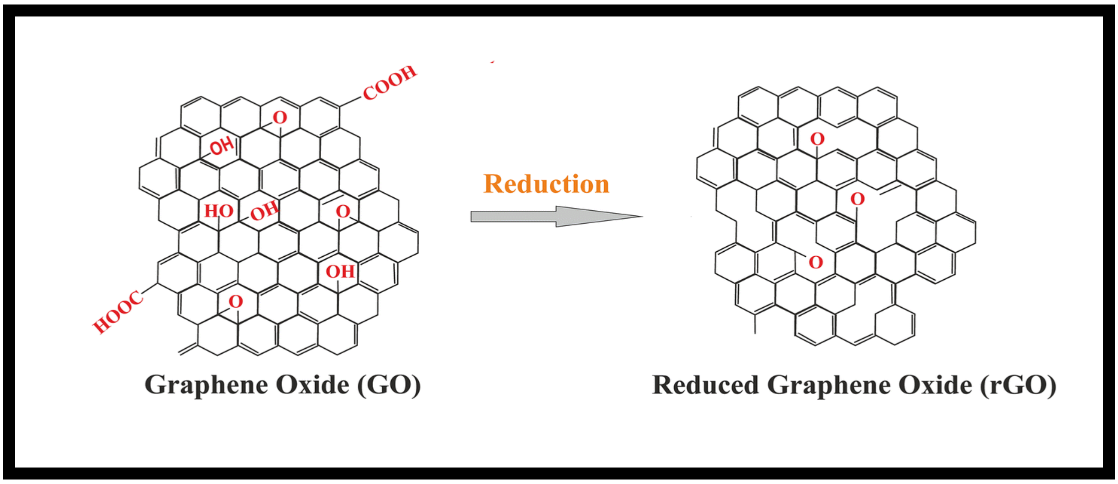

Figure 1.7 Structure of Reduced graphene oxide

Graphene oxide can be fuctionalized, chemically modified, reduced or converted to enhance its properties. The reduced graphene oxide (rGO) contains significant amount of residual oxygen, it is highly distorted, disordered and exists as few layers graphene. Reduction of GO can be done by various methods such as thermal, mechanical, electrochemical and chemical methods. Among all the methods, chemical reduction method is the most commonly used method to reduce GO into rGO. The chemical reduction can be done using reducing agents like hydrazine hydrate or sodium borohydride and the most important in reduction method is to obtain graphene like material both in terms of properties and structure. Thus the rGO can restore the conductivity of GO by the removing the oxygen functional groups and recovering the aromatic double bond. Thus the formed reduced graphene oxide is conductive which has more structural defects, functional groups and chemically active sites that allows it to act as a potential material for various applications like electrochemical, photocatalytic etc., [107]

1.7.6 Graphene based nanocomposites

Graphene based nanocomposites plays a major key role in modern science and nanotechnology. Moreover, tailoring of graphene-based nanocomposites exploits the superlative properties which show an enhanced performance in a large number of applications ranging from flexible packaging, semi-conductive sheets in transistors, memory devices, hydrogen storage, printable electronics, etc. Since oxygen-containing functional groups of graphene oxide can react easily with other organic substrates that change the hydrophilicity, hydrophobicity, or organophilicity properties of graphene, as required for functionalization with other matrices. For example, many modified GO sheets are readily dispersed in organic solvents for further functionalization, or for mixing with organic matrices to form new composite materials [108].

1.7.6.1 Functionalization of graphene oxide

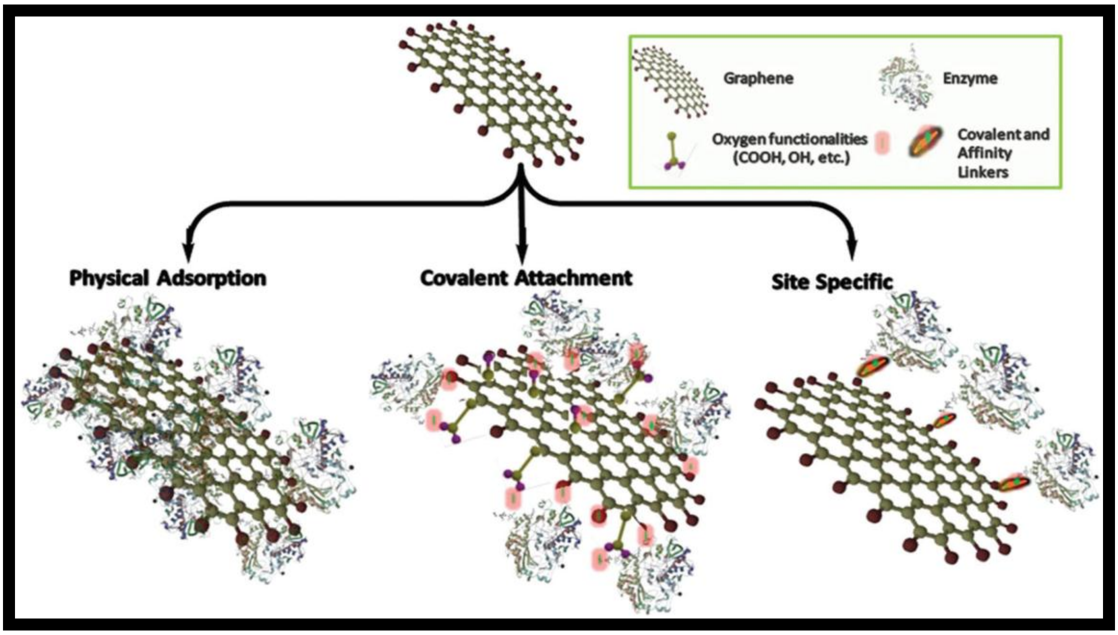

Figure 1.8 Functionalization of graphene oxide

The residual oxidized functional groups in graphene oxide are not sufficient to sustain the high surface area necessary for long-term stable dispersion in solvents.

Therefore, for many applications, it is necessary to tailor the surface of graphene in order to dissolve it in the required solvents or to increase the interaction between the matrix and graphene [109]. Thus functionalization of graphene results in the enlargement of specific area of electrode thereby leading to an enhanced current density. The graphene can be functionalized through a variety of interactions such as physical adsorption, covalent binding, entrapment, self-assembly and affinity as shown in the Figure 1.8. Covalent functionalization involves the chemical transformation of sp^2 to sp^3 hybridization by covalent addition. Organic functional groups attach covalently to either sp^2 bonds between carbon atoms or oxygenated groups present on graphene. Noncovalent functionalization involves the adsorption of small aromatic molecules onto the surface of graphene by physical interactions like Van der Waals, hydrophobic, or electrostatic interaction. Electrostatic interactions occur between the π–π stacking between the rings of graphene. In addition to this a variety of nanocomposite materials are rapidly emerging by incorporating other materials with graphene and functionalized graphene [110-111].

1.7.6.2 Applications of graphene based nanocomposites

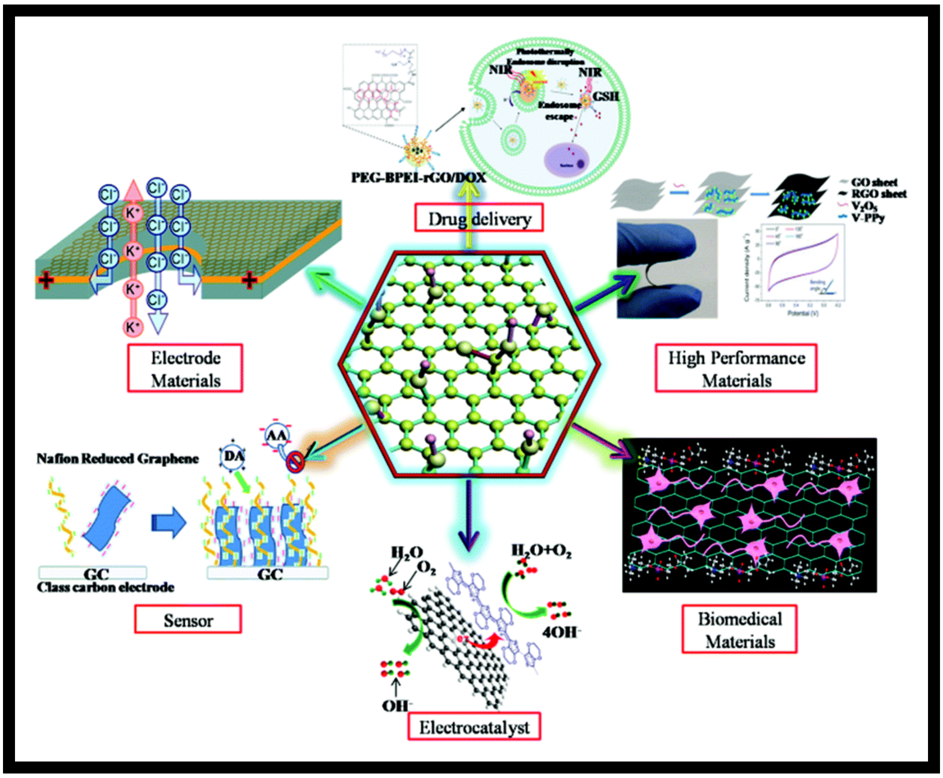

Figure 1.9 Applications of graphene based nanocomposites

Graphene based nanocomposites have been explored for a wide range of applications in many areas such as energy storage device, sensors, electromagnetic shielding, solar cells, liquid crystal devices, organic light emitting diodes, field emission devices, biomedical applications etc as shown in the Figure 1.9. They exhibit a moderate conductivity, high chemical stability and excellent electrochemical properties [112]. GO based composites are also found to be attractive for electrochemical applications due to its high surface area and good interaction with water and organic solvents. It is reported that GO facilitates the electron transfer of enzymes and proteins. Graphene based nanocomposites based electrodes are widely used in various electrochemical applications such as electrochemical sensors, electrochemiluminescence and electrocatalysis. Energy generation and storage on solar cells, which could be divided into those where graphene acts as the active medium and those that use graphene as a transparent or distributed electrode material. Graphene is used as a transparent electrode in dye-sensitized solar cells. Graphene had been extensively used in sensor and metrology [113]. Thus, it is natural to consider using graphene for sensor applications, from measurements of magnetic field to DNA sequencing and from the monitoring of the velocity of surrounding liquid to strain gauges. Since, graphene has a number of properties like large surface area, chemical purity and the facile functionalization that make it potentially promising candidate for bioapplications. Even in few cases, the ‘toxic’ graphene derivative can also be used potentially as a therapeutic for antibiotic/anticancer treatment. In science and purification technology graphene-based materials hold a great potential as adsorbents in decontaminating water due to their large surface area, layer like structure, diverse functionalities, facile preparation and low cost of treatment. Graphene and its composites have also been used in treating heavy metals such as (Ni, As, Cd etc), dyes, pesticide, antibiotics, oils and so on [114-115].

1.7.7 Polymer

Polymers are proved to be a good host matrix for enhasing the metal nanoparticles because they can act as both reducing as well as capping agents and also provide chemical stability environmental protection. The aim of this research project is to explore the potential use of chitosan by tailoring it through hydroxyl groups and amino groups that are capable of strongly interacting with various organic molecules for their remarkable uses in agriculture, electrochemical sensing and biological applications. Hence in pursuance of this, chitosan is blended with graphene oxide based nanomaterials to enhance its properties [116].

1.7.7.1 Chitosan

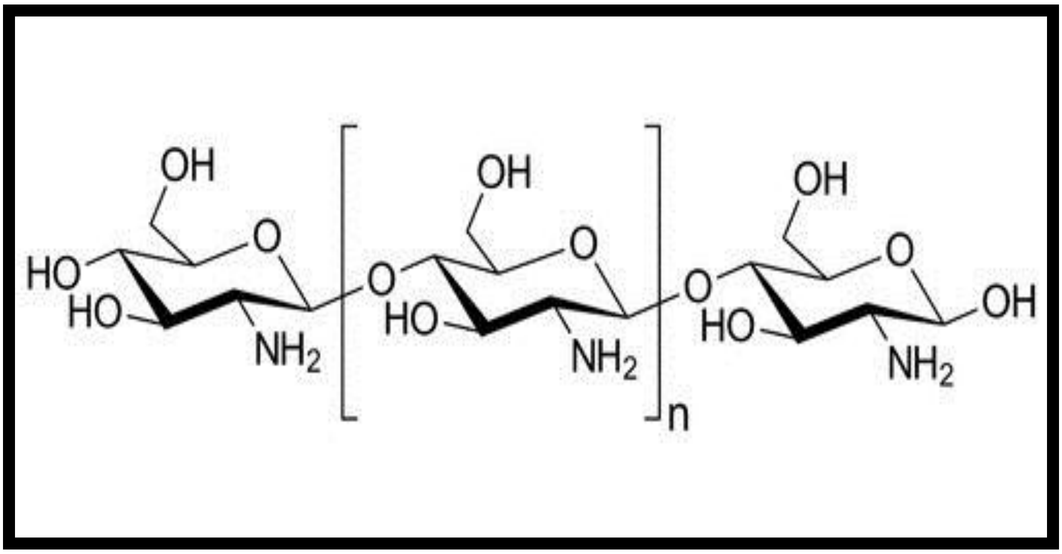

Figure 1.10 Structure of chitosan

Chitosan is a linear semicrystalline polysaccharide composed of β (1–4) linked-2-amino-2-deoxy-D-glucose and 2-acetamidoamino-deoxy-D-glucose as shown in the Figure 1.10. Its molecular structure has an amino group at C-2 position and 2 hydroxyl groups at C-3 and C-6 position, which form intermolecular hydrogen bonds that determine the stability of the polymer. Chitosan can be chemically modified through these amino and hydroxyl groups [117].

Chitosan is naturally found in the cell walls of some fungi. Chitosan is made by deacetylation of chitin. It is extracted from the exoskeletons generated by crustacean-processing plants from animals such as shrimp, lobsters, crabs and krill. Due to its unique biological characteristics like nontoxicity and biocompatibility, it has been gained abudant attention in the field such as drug delivery, supercapacitor, industrial additive and sensing applications [118].

1.7.7.2 Chitin to chitosan

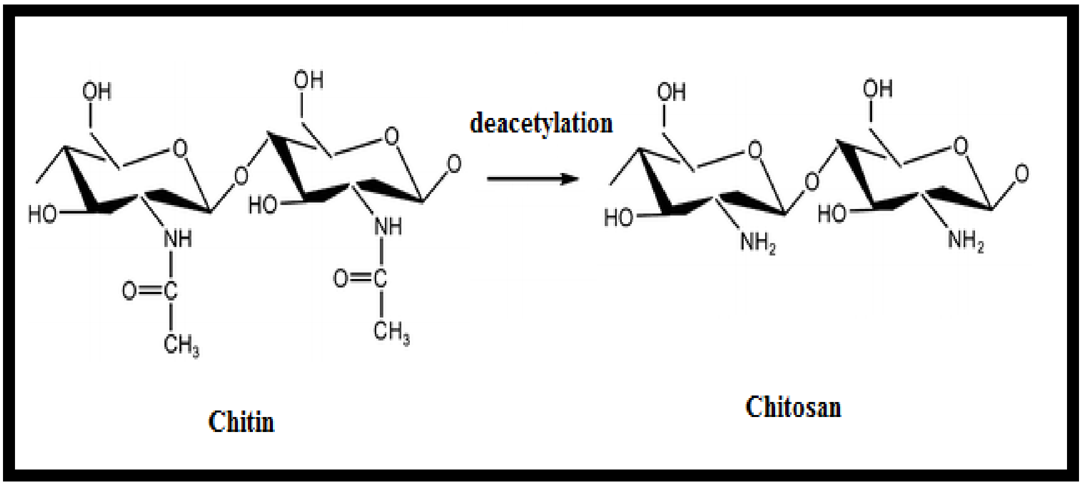

Figure 1.11 Chitin to chitosan

Chitin is converted to chitosan by chemical or enzymatic methods at which both the processes are based on the deacetylation of chitin at which the acetyl groups are removed from *N*-acetylglucosamine to d-glucosamine units that contain free amino groups which increases the solubility of the chitosan in aqueous media as shown in the Figure 1.11. Chemical methods are used widely because of their low cost and suitability to mass production. The chemical purification of chitin is done by demineralizing the wastes by applying dilute HCl and then deproteinized in a dilute aqueous solution of NaOH or KOH [119-120].

1.7.7.3 Physiochemical Characteristics

Chitosan is soluble in dilute acid solutions below pH 6 and insoluble in water and in alkaline solutions. Organic acids like acetic, lactic and formic acids are generally used for dissolving chitosan whereas 1% acetic acid solution is the most commonly used solvent for dissolving chitosan [121]. The most important parameter influencing the characteristicts of chitosan is the degree of deacetylation (DDA) and molecular weight. DDA is the proportion of d-glucosamine units relative to the total number of units (*N*-acetyl-d-glucosamine plus d-glucosamine) that influences the properties and applications of chitosan. Generally, the DDA of chitosan is in the range of 60%–98%. The rate of deacetylation influences the solubility, hydrophobicity and its capability to interact with polyanions molecules. Chitosan at lower molecular weight have lower deacetylation, greater solubility and fast degradation process compared to that of higher molecular weight of chitosan. Thus the molecular weight of commercially obtained chitosan ranges from 3800 to 20,000 Daltons [122-123].

1.7.7.4 Biological properties

The unique properties of chitosan such as biocompatibility, biodegradability, non-toxicity, high humidity absorption analgesic, antitumor, hemostatic, hypocholesterolemic, antimicrobian and antioxidant have gained a great deal of interest for researchers which make them suitable for versatile applications in medical and pharmaceutical sector. Chitosan with low molecular weight of chitosan can penetrate easily into the cell membrane of a microorganism and thereby prevents the growth of the cell by inhibiting DNA. The acetyl groups and the length of polymer chain can also affect the biodegradation kinetics of chitosan. The cationic nature of chitosan persuades its biological and antimicrobial activity. In addition, the polycationic nature of chitosan attracts the anionic components in the cell, thus resulting in the changes in permeability by inducing leakage of intracellular components that leads to the cell death. Moreover, chitosan adsorbs the electronegative substrate in the cell of microbe proteins and thereby disrupts the physiological activities of the microorganism leading to the death of the cells. It has also been observed that chitosan with a high DD (97.5 %) can lead to higher positive charge density which confers a stronger antibacterial activity than that of low DD (83.7 %) [124-125].

1.7.8 Metallic nanoparticles

The novel electrocatalytic behaviour of metal or metal oxide nanostructures combines the features of electrochemistry and chemical reactivity. Metal or metal oxide nanostructures have been studied intensively in the last few years because of their unusual physical and chemical properties owing to their extremely small size, large specific surface area and a number of promising applications such as drug delivery, medicine, electronics, bio sensors, chemical sensors, catalysts, fuel cells, batteries and solar cells [126].

In view of the imperative features of metal or metal oxides nanostructures, much research has been concentrated on metal and metal oxide based electrochemical sensor since most of the literature has reported that metal or metal oxide-modified interfaces have enhanced the electrochemical signaling of target molecules. Thus integration of graphene oxide with different metal or metal oxide nanostructures enhances the electrochemical catalytic activity of the nanocomposites. The hybrid nanocomposite provides larger electrochemically active surface area which facilitates the adsorption of more biomolecules and expedites the electron transfer between the electrode surface and target, consequently leads to a sensitive and fast current response [127].

1.7.9 Zinc oxide

During last few decades, semiconducting materials attracted researchers for its unique properties and versatile applications. It is a semiconductor material belongs to II-VI compounds. It is an n-type semiconductor of wurtzite structure with good transparency and high electron mobility. They have a wide band-gap of 3.37 eV with large exciton binding energy of 60 MeV. It is nontoxic, biocompatible and an inexpensive luminescent material with exceptional electrical and optical properties. It decomposes into zinc vapour and oxygen only at around 1975°C, reflecting its considerable stability. They are not only stable but also a safe and biocompatible material. Owing to their extraordinary properties, it has wide range of applications in transparent electronics, piezoelectric devices, chemical sensors, spin electronics, bio imaging and drug delivery [128-129].

1.7.9.1 Crystal structures of ZnO

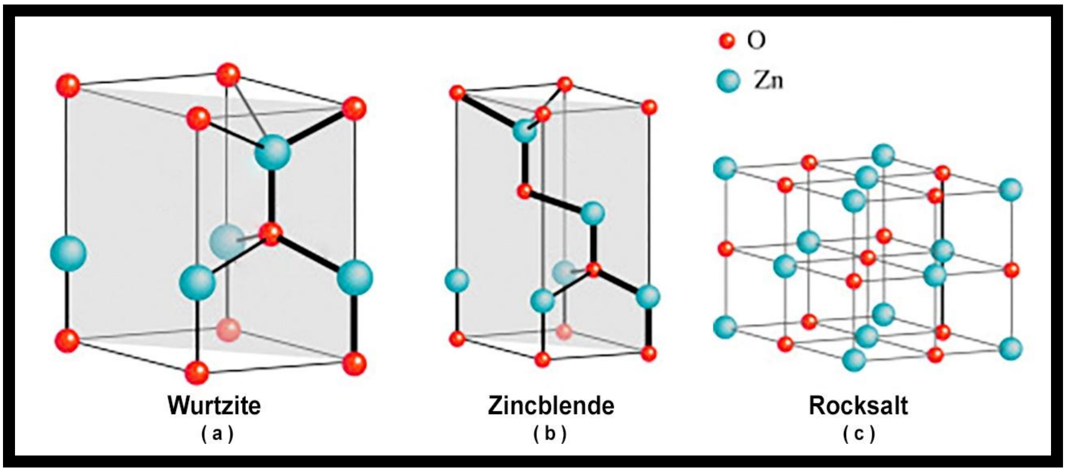

Figure 1.12 Crystal structures of ZnO

ZnO is a semiconductor material at which each anion is surrounded by four cations at the corners of a tetrahedron with a tetrahedral bonding configuration, corresponds to the sp^3 covalent bonding as shown in the Figure 1.12. The lattice parameters are a = 3.2 Å and c = 5.2 Å. The c/a ratio for ZnO is about 1.603, which is slightly less than the ideal value 1.633. The three possible crystal structures are hexagonal wurtzite, zinc blende and rock salt. The most stable structure under thermal equilibrium is wurtzite structure. The cubic zinc blende structure of ZnO can be stabilized only by growth on cubic substrates such as ZnS, GaAs/ZnS, Pt/Ti/SiO2/Si etc., The rock salt or rochelle salt structure of ZnO is obtained only at relatively high pressures [130-131].

1.7.9.2 Mechanical properties

ZnO is a soft material with thickness of about 4.5 on the Mohs scale. Its elastic constants are relatively smaller than those of III-V semiconductors. Consequently, ZnO has the highest piezoelectric tensor compared to GaN and AlN. This property of ZnO makes it technologically important and also paves the way for many piezoelectrical applications that require a large electromechanical coupling [132].

1.7.9.3 Electronic properties

The distinctive features of the material include non-stoichiometric defect structure and large direct band gap with high optical transparency in the visible region. It has a relatively higher breakdown voltages that makes it to sustain large electric fields, lower electronic noise, high-temperature and high-power operation. Thus the band gap of ZnO can be tuned to ~3– 4 eV by alloying it with magnesium oxide or cadmium oxide. Most of the ZnO has n-type character, even in the absence of intentional doping. The successful n-type doping is achieved easily by substituting Zn and O with either group-III elements like Al, Ga, In or with group-VII elements such as chlorine or iodine [133].

1.7.10 Copper oxide

Copper (II) oxide or cupric oxide (CuO) is the inorganic compound. Copper oxides have two stable forms: cuprous oxide (Cu_2O) and cupric oxide (CuO). Both oxides have very different colours, crystal structures, physical properties and electrical properties. It is a semiconductor metal oxide which is nontoxic, low cost and has abundant source materials. Owing to its excellent optical, electrical and magnetic properties it has gained a renewed interest in various applications such as supercapacitors, near-infrared filters, magnetic storage media, sensors, catalysis, semiconductors, drug delivery etc. optoelectronic properties. As a mineral, it is known as tenorite and paramelaconite [134-135].

1.7.10.1 Structure of CuO

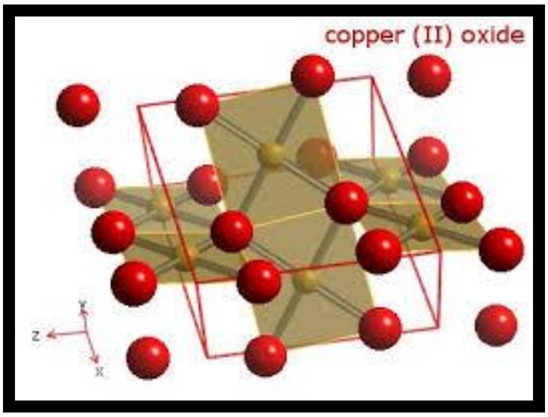

Figure 1.13 Crystal structures of CuO

Copper (II) oxide belongs to the monoclinic crystal. The copper atom is coordinated by four oxygen atoms in an approximately square planar configuration. The Lattice constants are a = 0.47 nm, b = 0.34 nm, c = 0.51 nm and β = 99.54. The copper atom is coordinated by four coplanar oxygen atoms at the corner in the form of rectangular parallelogram. The oxygen atom is coordinated to four copper atoms in the form of a distorted tetrahedron as shown in the Figure 1.13 [136].

1.7.10.2 Physiochemical properties of CuO

Copper oxide (CuO) is a black solid with a density of about 6.4 g/cm^3. It have attracted much attention due to its unique physical and chemical properties such as high specific surface area, high solar absorbancy. It is a p-type semiconductor with a band gap of 1.7eV. It has a high melting point of about 1330ºC. It is insoluble in water and can be easily mixed with polarized liquids and polymers. It is an amphoteric substance, which means it can act as an acid or a base. It is non-flammable. They are relatively cheap and relatively stable in terms of both chemical and physical properties. It is malleable, ductile and a good conductor of electricity and heat [137-138].

1.7.11 Silver

Silver is an important material that has received considerable attention due to its unique properties like optical, electrical and magnetic properties. Because of their high surface area to volume ratio and high active surface they exhibit remarkable and outstanding properties, such as increased catalytic activity which have wide range of applications like antimicrobial applications, biosensor materials, composite fibers, cryogenic superconducting materials, cosmetic products, and electronic components [139].

1.7.11.1 Structure of Ag

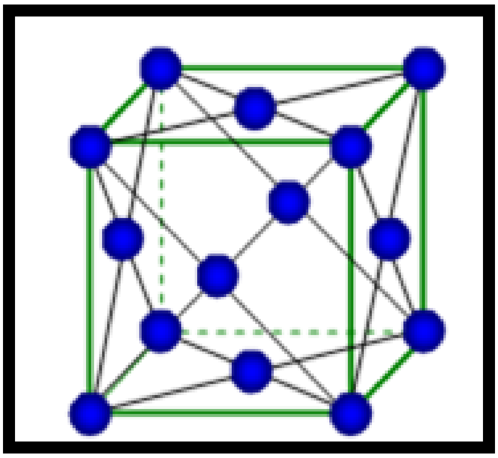

Figure 1.14 Structure of Ag

Silver belongs to the face centered cubic system. The structure of silver is shown in the Figure 1.14 [140].

1.7.11.2 Physiochemical properties of Ag

Silver is an interesting material for research among all the other metals due to its outstanding electrical, thermal and optical properties. It is a chemical element with symbol Ag that belongs to the group 11 of periodic table and its atomic number is 47. It is a rare, soft, lustrous, very ductile and malleable metal. It is soluble in water and forms complex comounds. It does not react with O_2, N_2, or H_2 at normal temperatures**.** It has the highest electrical conductivity with minimum interaction opposition compared to other metals, but it is not widely used for electrical purposes as it is very expensive. They are not chemically active however nitric acid and hot concentrated sulfuric acid will easily react with it. It also occurs in minerals such as argentite and chlorargyrite [141-142].

1.7.12 Gold

Gold nanoparticles as a colloidal dispersion have been considered as a promising candidate for domestic, scientific, and industrial applications. Compared to other metals gold NPs are highly stable and easy to functionalize. They have unique chemical, physical, and optical properties. Due to their large surface area, low toxicity, controllable size, biocompatibility and convenient surface conjugation with biomolecules they have applied in the areas of electronics, catalysis, biosensor, biomedicine and pharmaceutical applications [143].

1.7.12.1 Structure of Gold

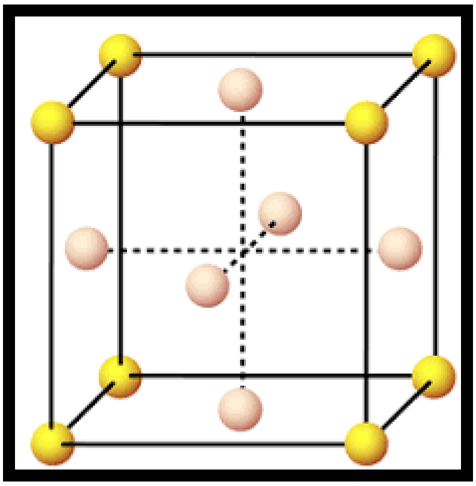

Figure 1.15 Structure of Au

Gold belongs to the face centered cubic system. The structure of gold is shown in the Figure 1.15 [144]

1.7.12.2 Physiochemical properties of Au

It is the most malleable among all the other metals and good conductor of heat and electricity. It is a heavy metal with density of about 19.3 g/cm^3. They can be beaten into very thin sheets in the form of leaf to make it semi transparent. Thus the semi transparent sheets reflect infra red light which may be applied in infrared shields as a visors of heat-resistant suits. They possess a distinctive optoelectronic property like localized surface plasmon resonance (LSPR). Due to their remarkable optical property they display a characteristic colour which mainly depends strongly on their size, shape, local environment, dielectric constant and degree of aggregation.The specific physiochemical properties of Au NPs make them as an excellent scaffold for electrochemical sensors fabrication [144].

1.7.13 p-Aminophenol

Aminophenols and their derivatives are of great commercial importance which is used as intermediates in the photographic, pharmaceutical, and chemical dye industries. They are amphoteric and can behave either as weak acids or weak bases. Based on the position of amino and hydroxyl groups, they exists in three possible isomeric forms [65].

p-Aminophenol (p-AP) is used as an intermediate in the manufacture of fur, hair dyes paracetamol, acetanilide, phenacetinsall analgesic and antipyretic drugs. It is also used as a developer in photography, wood stain, imparting a rose like colour to timber and in chemical dye industries. In general, p-AP is irritants and their toxic hazard rating is slight to be moderate. In pharmaceutical preparations of paracetamol, p-AP is obtained as the primary hydrolytic degradation product which is dangerous to living things causing serious teratogenic effect and nephrotoxicity. It is a selective nephrotoxic agent that interrupts the proximal tubular function. In order to prevent the harmful effects of ingestion, its presence in the drug substances is limited to a level of 50 ppm (0.005% w/w) by the European and United States of pharmacopeia. The repeated contamination of p-AP may cause general itching, skin sensitization, dermatitis and allergic reactions. Immunogenic conjugates are spontaneously produced upon exposure to p-AP. The methemoglobin formation with subsequent cyanosis is another possible complication. Inhalation of p-AP can cause irritation to the mucosal membranes and may precipitate allergic bronchial asthma. In addition, releasing of p-AP from industrial waste waters into streams and rivers, they tend to deplete the capacity of these environments and sustain aquatic life. Further chlorination of drinking water may enhance the toxicity of p-AP present as pollutants. Moreover, p-AP poses a risk of irreversible effects on human health, specifically the blood and kidneys. Hence, trace level detection of p-AP in the surrounding substances is essential for both environmental and human safety aspects. Numbers of methods are used for the determination of p- AP such as spectroscopy, fluorescence, capillary electrophoresis, micellar electro kinetic chromatography, nuclear magnetic resonance spectroscopy analysis, electrochemical etc.,. Among these methods, electrochemical methods are considered to be more prefereable and widely used due to their low-cost, simplicity, rapid detection, high sensitivity and selectivity [68-69].

1.8. CHARACTERIZATION TECHNIQUES

Instrumentation helps us to understand the specific properties of the substance, to be studied in a rapid manner accurately as well as reliable to understand measured values. The synthesized nanocomposites are subjected to various studies. The structural, surface, compositional studies and electrochemical properties of the prepared nanocomposites are done using sophisticated techniques such as X-Ray Diffraction (XRD), Scanning Electron Microscope (SEM), Fourier Transform Infra Red Spectroscope (FTIR), Energy Dispersive X-Ray spectrometer (EDX), High Resolution-Transmission Electron Microscope (HR-TEM) and Electrochemical system.

1.8.1 Fourier transform infrared spectroscope (FT-IR)

Fourier Transform Infrared Spectroscopy (FT-IR) is used to investigate the molecular structures and bonding interactions of the prepared nanocomposites. The functional groups can be identified by measuring the spectrum of absorbed radiation [145].

The infrared spectra are recorded using a perkin Elmer IR spectrometer. FT-IR spectroscopic analysis is recorded in the range from far infrared region (400 cm^{-1})

to the mid infrared region (4000 cm^{-1}). This spectrometer uses infrared light and the spectrum depicts the transmission and absorbance of light for all the infrared wavelengths. When the sample is irradiated by a broad spectrum of infra-red light, it absorbs the radiation and the chemical bonds tend to vibrate at characteristic frequencies. The radiation absorbed at particular frequency produces a spectrum that can be used to determine the functional groups and compounds, since the chemical bonds absorb infrared energy at specific frequencies. The plot of the IR transmission versus frequency is its "fingerprint" which can be compared to reference spectra to classify the material [146].

1.8.2 X-Ray diffraction analysis (XRD)

The crystalline phases of the prepared nanocomposites are studied using XRD analysis. In a crystalline solid, the constituent particles like atoms, ions or molecules are arranged in a regular order. An interaction of a particular crystalline solid with X-rays helps in investigating its actual structure, orientation, composition, phases, internal lattice strain and particle size. Crystals are found to act as diffraction gratings for X-rays and this indicates that the constituent particles in the crystals are arranged in planes at close distances in repeated patterns [147]. The phenomenon of diffraction of X-rays by crystals is studied by W. L. Bragg and his father W. H. Bragg in 1913.

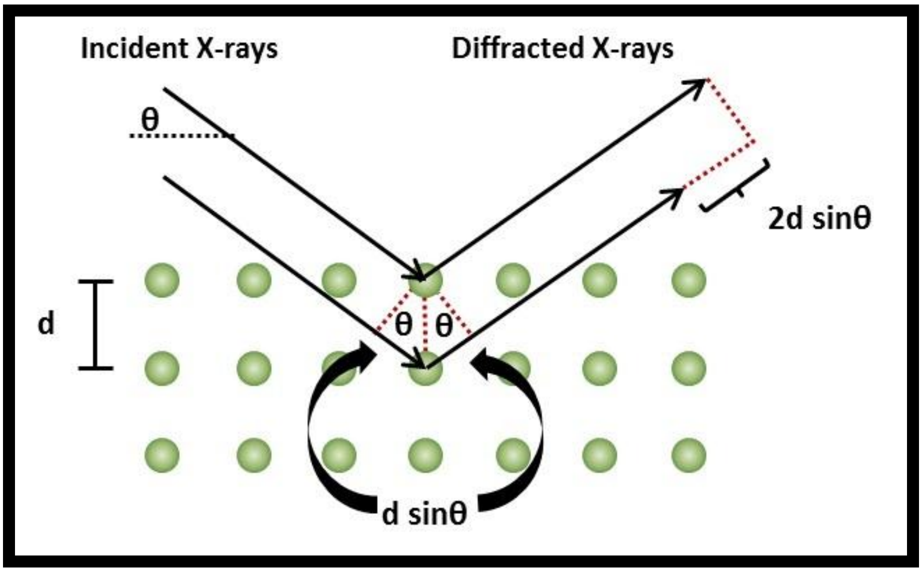

Figure 1.16 Schematic representation of X-ray diffraction

The X-ray diffraction patterns of the prepared nanocomposites are carried out using a Bruker D8 Advance powder X-ray diffractometer equipped with a Våntec-1 detector which is operated at 40 kV and 30 mA with Cu $K\alpha$ radiation. The finely powdered prepared nanocomposites are placed on the sample holder and X-Rays are directed towards the sample. These X-Rays interacts with the atoms in the nanocomposites through constructive or destructive manner, when conditions satisfy Bragg's Law as depicted in Figure 1.16

$$\mathbf{n\lambda=2d \sin \theta}$$

where, λ = wavelength of X-ray (Å),

θ = incident angle.

d = interlayer distance.

n = order of diffraction

The diffracted waves emitted by the array of atoms have the same frequency as that of incident rays. Thus the diffracted waves are then scanned, detected and recorded [148].

1.8.3. Scanning electron microscopy

The surface morphology of the prepared nanocomposites is characterized using Scanning Electron Microscope analysis. The schematic of Scanning electron microscope is shown in the Figure 1.17. It is a type of electron microscope that produces high-resolution images of the surface of the sample. SEM equipped with diffracted backscattered electron detectors are used to examine the crystallographic orientation in materials. The SEM images reveals about the morphology, structure and composition of the nanocomposites. The surface of the sample can be clearly seen using three dimensional SEM images [149].

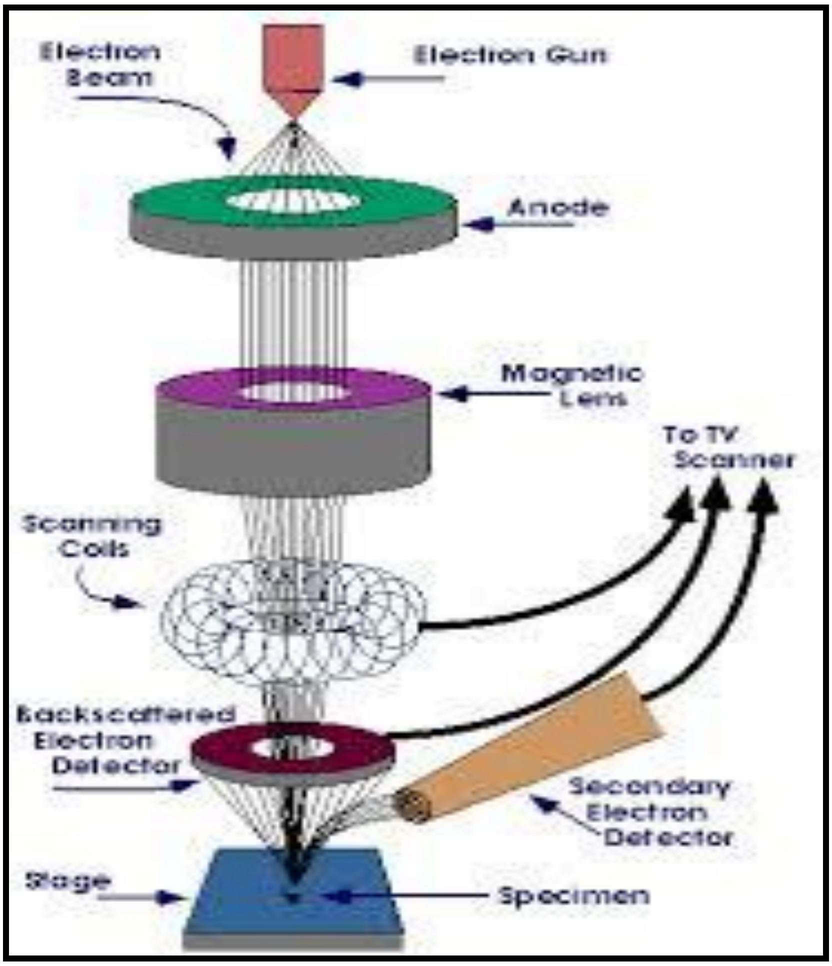

Figure 1.17 Schematic diagram of Scanning electron microscope

In this present work, Zeiss FESEM 1530 scanning electron microscope is used for the analysis of surface morphology of prepared nanocomposites. It is operated in the range of 30 keV and the areas are scanned in the range of 1 cm to 5 microns with its magnification ranging from 20 X to 30,000 X and its spatial resolution of about 50 to 100 nm. The electron beam from the tungsten filament is directed towards the sample with an accelerating voltage of about 1 to 30 kV. This electron beam gets diverged and passes through a pair of electro-magnetic lenses and interacts with the sample and thus the interaction of electron beam with the sample results in the exhibition of secondary electrons, backscattered electrons and various energies of characteristic X-rays. The secondary electrons and the backscattered electrons are scanned and detected to investigate the surface morphology, crystallography and composition of the sample [150].

1.8.4. Energy Dispersive X-ray Analysis

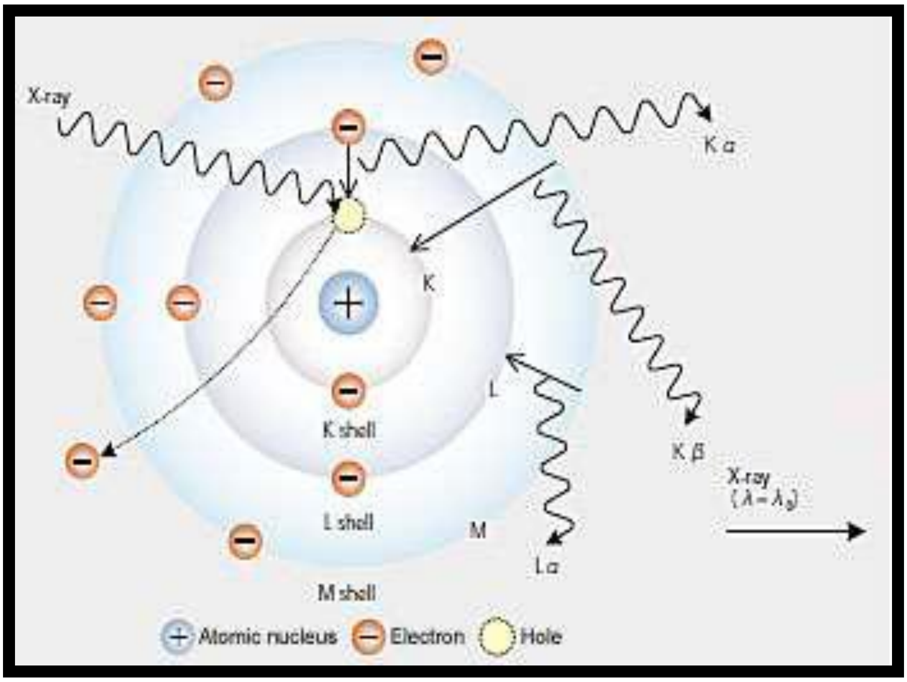

Figure 1.18 Schematic diagram of EDAX

The elemental presence and composition of the elements are further investigated using Energy dispersive X-ray characterization (EDAX) technique. It is performed along with scanning electron microscope. The schematic representation of EDAX is shown in the Figure 1.18. The fundamental principle of EDAX analysis is the interaction of some source of excited X- rays with the sample. Thus each element has its own atomic structure resulting in the unique set of X-ray emission spectrum. A high energy beam of X-Rays are used to excite the emission of characteristic X-Rays from the sample. When an atom is at rest, the sample holds the unexcited electrons in the discrete energy level. Thus the incident beam excites an electron in the inner shell by creating a hole and an electron from the outer shell fills the hole. The energy released during this process will be in the form of X-Rays. The energy and number of the X-rays emitted from the sample is measured by an energy-dispersive spectrometer which gives raise to the detection of the elemental composition of the sample [151].

1.8.5 High-resolution transmission electron microscope

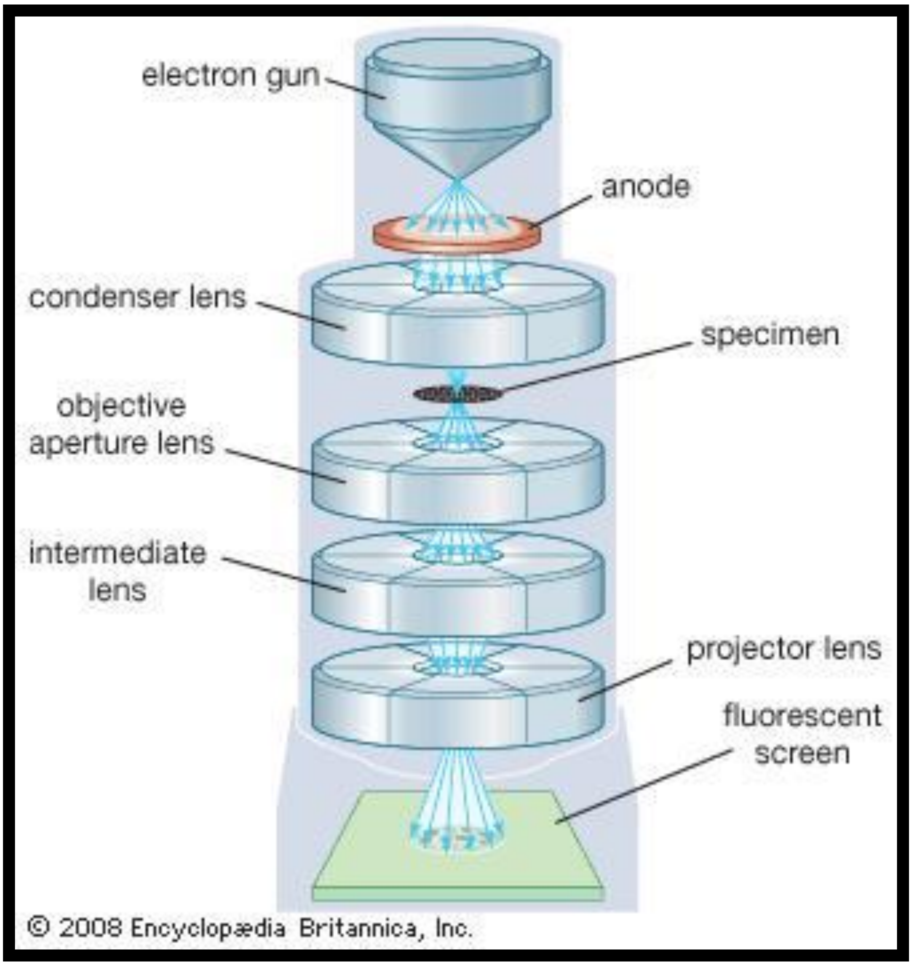

Figure 1.19 Schematic diagram of HR-TEM

Transmission Electron Microscopy (TEM) is extensively used for measuring the particle size of nanoparticles. The principle of operation of TEM is same as that of the optical microscope, but in this case a beam of electrons is used instead of light.

In this present work, JEOL 2100 F model is used to generate higher resolution transmission electron microscope images. When monochromatic electron beam strikes the sample, some of the electrons are scattered and some are transmitted. The transmitted electrons are then passed through an objective lens which gives an inverted image. An objective aperture is placed at the back of the objective lens to form an image. The first image generated by the objective lens is further projected onto a phosphorus coated screen which emits visible light. The brighter areas of the image indicates the passage of more number of electrons whereas the darker areas represent that only few electrons have passed through it. Some other effect produced by striking electron is that it emits X-ray photons, Auger electrons, secondary electrons, backscattered electron, etc. Many of these effects are used for characterizing the specimen as shown in the Figure 1.19. Thus TEM record the information carried by transmitted electrons, unscattered as well as elastically and inelastically scattered electrons [152-153].

Electron diffraction pattern produced in transmission in the electron microscope can be of three different types.

- Ring pattern – polycrystalline
- Spot pattern – single crystal region of the species
- Kikuchi line pairs – bands in electron diffraction

Spot and Kikuchi patterns are taken from a specific area of the specimen and are known as “Selected area diffraction pattern”. De Broglie proposed that particles could have both particle and wave nature. He attributed that wavelength (λ) associated with the moving particle of velocity v is given by

$$\boldsymbol{\lambda = h/m\nu}$$

Where, h - Planck’s constant,

m- mass of an electron

ν - velocity of an electron [154].

1.8.6 Electrochemical sensors

A sensor is a device that is used to detect the presence of analyte and collects the information that converts it into corresponding signals which can be recorded. They are used widely in many fields such as medical diagnostics, food, pharmaceutical labs and environmental analysis. They are broadly classified into physical sensors, biosensors and chemical sensors. Among them, chemical sensor is a device which responds selectively to a particular analyte by means of chemical reaction that can be used for the qualitative and quantitative determination of analyte [155].

A chemical sensor consists of active sensing material which works as receptor and signaling unit. The receptors are designed in such a way that it should provide fast and reversible binding to the analyte. When an analyte binds to the receptor part, the signal observed by the reporter changes. Similiarly, the reporter group is chosen by the electrochemical properties that can be amended by consequent receptor-analyte interaction. Hence, the output of electrochemical sensors is monitored and the presence of certain analytes can be determined. Thus based on the transducer type, the chemical sensors are broadly classified into electrochemical, spectroscopic, mass and heat sensors. A good sensor should be selective for a particular analyte and able to monitor the concentration of analyte varying from very low to high concentrations [156].

Electrochemical sensors are device that alters the response of the chemical interaction between sensor device and analyte into applicable analytical signal. Electrochemical measurements can be done under steady conditions. The immediately resulted analytical signal provides the combined features of electrochemistry and the chemical sensors. The modes of operation of electrochemical sensors depend on the selectivity and sensitivity of a particular sensor, since the mode of operation greatly affects the potential applied for electrochemical sensors. Recently, electrochemical sensors have gained much interest since they can be potentially utilized in several fields such as in environmental monitoring, clinical assays, quality monitoring as well as in medical applications. They have numerous advantages in terms of sensitivity, selectivity, quick response time. In comparison to the other techniques, electrochemical sensing methods are usually favoured due to their simple set up and electronic requirements. Moreover, easy maintenance and calibration are the important key features of these sensors [157].

1.8.6.1 Experimental set up and instrumentation

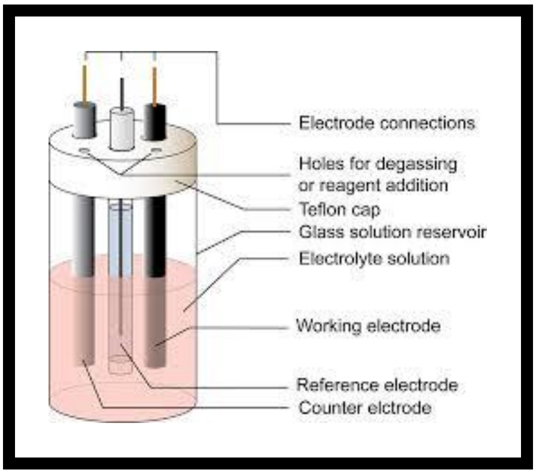

Figure 1.20 Electrochemicl set up

The most commonly used system in electrochemistry is three-electrode cell setup inorder to avoid the passage of current through the reference electrode. It consists of working electrode (WE), reference electrode (RE), counter electrode (CE) and supporting electrolyte as shown in the Figure 1.20. The WE is an ideally polarizable electrode where the electrode shows a large change in potential even at a low potential. RE is a nonpolarizable electrode at which it has a fixed potential and CE is a current conducting electrode. In general, the electrochemical measurements are done in the presence of the supporting electrolyte in order to provide electrical conductivity between the electrodes. In this electrochemical circuit the current flows between the WE and the CE. The potential difference between the WE and CE is measured at the RE and the resulting current is directly sent to the computer [158].

Working electrode

Figure 1.21 Working electrode

The working electrode can be referred to as either cathodic or anodic depending on the redox process on the electrode. Most common working electrodes used are inert electrodes like gold, silver or platinum, glassy carbon or pyrolytic carbon, mercury drop, film electrodes and mercury electrodes as shown in the Figure 1.21. Among all these glassy carbon electrodes (GCE) are widely used due to its advantages like low cost, pretreatment by polishing with metallographic paper, increased reversibility for several redox couples and reactions that involve subsequent proton transfer [159].

Counter electrode

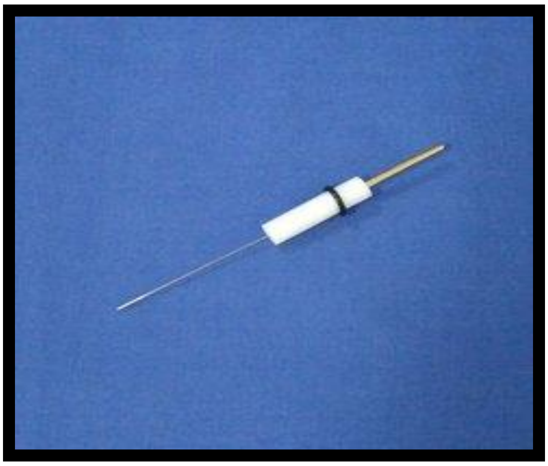

Figure 1.22 Counter electrode

Platinum electrodes are the most widely used auxiliary or counter electrodes in molten salt, aqueous and non-aqueous media. It is in the form of coils or thin foils as shown in the Figure 1.22. In two electrodes system, only reference and working electrode is used, at which the current flowing through the reference electrode causes a change in its potential. The purpose of counter electrode is to complete the circuit. Thus in case of three electrodes system, the current flows between the working electrode and counter electrode. The electrode area of the counter electrode must also be larger than that of working electrode to ensure that the platinum electrode does not control the process of working electrode [160].

Reference electrode

Figure 1.23 Reference electrode

A reference electrode is an electrode that has a stable and known electrode potential. When an external potential is applied to the working electrode, the reference electrode potential should not change and must be insensitive to the composition of the analyte solution. The most commonly used electrodes are standard hydrogen electrode (SHE), silver-silver chloride electrode (Ag/AgCl) and calomel electrode as shown in the Figure 1.23[161].

1.8.6.2 Cyclic voltammetry

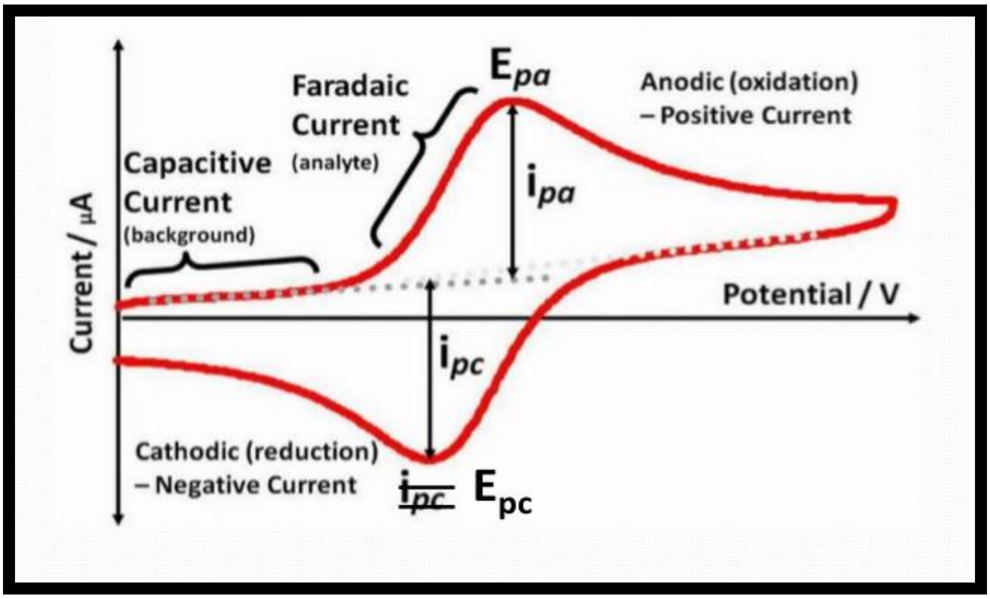

Figure 1.24 Cyclic voltagramm curve

Cyclic voltammetry (CV) is the most commonly used electroanalytical technique to study redox processes and electrochemical properties of analytes in buffer solution. The general principle of the voltammetric techniques is that the application of a potential (E) to an electrode and observing the resulting current (I) which passes through the electrolyte. In many cases, the applied potential is varied or the current is monitored over a period of time (t) [162]. Thus all voltammetric techniques can be described as a function of E, I, and t. The CV studies are carried out by scanning the potential of the working electrode in a cyclic manner and switching it in reverse. The flowing current can be measured through the working electrode. The resultant trace of current against potential is termed as a voltammogram. During cyclic voltammetry measurement, the potential is ramped from an initial potential (Ei) to a more negative potential, but at the end of its linear sweep the direction of the potential scan is reversed, usually stopping at the Eo. The potential is usually measured between the reference electrode and the working electrode and the current is measured between the working electrode and the counter electrode. This data is then plotted as current versus potential as depicted in the Figure 1.24

When a potential is applied, a redox peak current is obtained for an analyte. The current increases as the concentration of analyte increases, but then decreases when the concentration of the analyte is depleted close to the electrode surface. If the redox process is reversible, then reversing the applied potential makes it reach a potential that re-oxidizes the product formed in the first reduction reaction, thus producing a current of reverse polarity from the forward scan. The oxidation peak usually has the same shape as that of the reduction peak. As a result, the information about the redox potential and the electrochemical reaction rates of compounds are obtained. Moreover if the transfer of electrons at the surface is fast, then the anodic and cationic peak current will be proportional to the square root of the scan rate current which is limited by the diffusion of species to the electrode surface. Thus the important parameters in a cyclic voltammogram are the cationic and anodic peak potentials (Epc, Epa) and cationic and anodic peak currents (Ipc, Ipa) respectively [163-164].

1.9 SCOPE OF THE WORK

Recently, graphene oxide based nanocomposites have been receiving considerable attention as a result of their unique properties that leads to tremendous applications in various fields like optics, electronics, biomedicine, magnetic, mechanics,catalysis and energy science. Further, on compositing it with metals, metal oxides, polymers, semiconductor etc., will improve their existing properties. Hence, the main scope of the present work is

- To synthesize Graphene oxide by modified hummer’s method.
- To functionalize graphene oxide by polymer.
- To embellish various concentrations of metal, metal oxides on polymer functionalized graphene oxide.
- To characterize the synthesized nanocomposites for its structural and morphological properties using FT-IR, XRD, SEM, EDAX, HR-TEM and SAED.
- To utilize the prepared nanocomposites in sensing and biomedical applications.
- To investigate electrochemical detection of p-Aminophenol
- To study the effect of Antibacterial and anticancer activity.

The research methodology used to accomplish the objectives

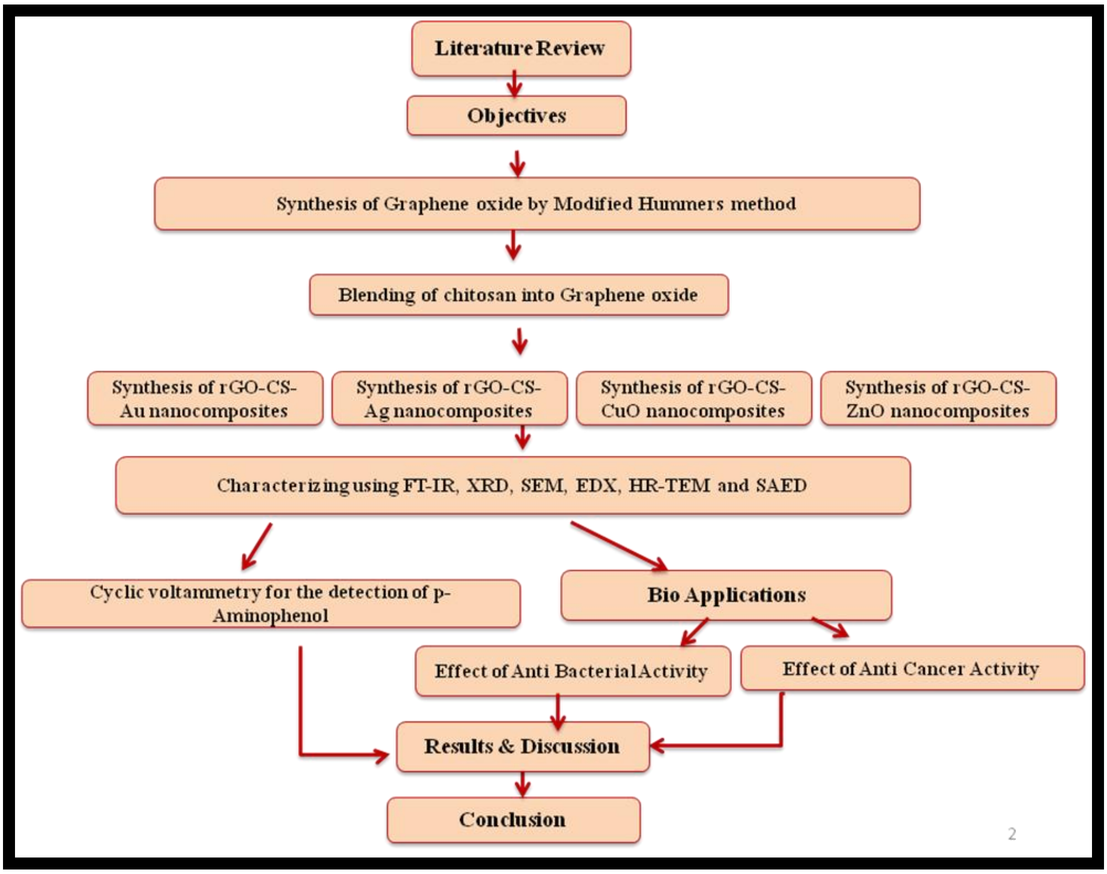

Figure 1.25 Methodology

1.10 ORGANIZATION OF THESIS

The present thesis essentially comprised of eight chapters. The content of each chapter has been briefly described below.

CHAPTER I describes the importance of Nanoscience and Nanotechnology and its vital role in various fields. It deals with the introduction and properties of graphene oxide, chitosan, metal and metal oxides for various applications. It discusses the detailed review of relevant literature which opens up the way for the development of novel nanocomposites for various applications. It also outlines the instruments used for the characterization of synthesized nanomaterials.

CHAPTER II deals about the synthesis of graphene oxide by Modified Hummer's method in which graphite is treated with a mixture of very strong oxidizers such as sulphuric acid, sodium nitrate and potassium permanganate. The blending of chitosan into reduced graphene oxide is achieved by chemical precipitation method.

The structural, morphological and functional properties of the nanocomposites are investigated by X-Ray diffraction (XRD), scanning electron microscopy (SEM), energy dispersive X-ray (EDAX) and Fourier Transform spectroscopy (FT-IR). The electrochemical properties of the nanocomposites are studied using cyclic voltammetry analysis.

CHAPTER III describes the influence of different concentrations (0.002M, 0.004M, 0.006M, 0.008M and 0.01M) of zinc oxide nanoparticles incorporated on the surface of rGO-CS nanocomposites. The high crystalline diffraction peaks of zinc oxide nanocomposites are in well agreement with the JCPDS card no (36-1451). The investigation of cyclic voltammetry studies for the detection of p-Aminopheol at different pH of phosphate buffer solution and at different scan rate is also studied. The synthesized nanocomposites showed the enhanced electro catalytic activity towards the detection of p-Aminophenol.

CHAPTER IV illustrates the synthesis of various concentrations (0.002M, 0.004M, 0.006M, 0.008M and 0.01M) of copper oxide nanoparticles on the surface of rGO-CS nancomposites. This chapter figures out the investigations carried out to examine the properties such as functional, structural, morphological, and elemental composition of synthesized nanocomposites by FT-IR, XRD, SEM, EDAX techniques. The investigation of cyclic voltammetry for the detection of p-Aminophenol at different pH of phosphate buffer solution and at different scan rate is also studied.

CHAPTER V describes the synthesis of various concentrations of silver nanoparticles incorporated on the surface of chitosan blended reduced graphene oxide nanosheets. The structural, morphological and functional properties of the prepared nanocomposites are examined. The influence of various concentrations of the silver nanoparticles (0.002M, 0.004M, 0.006M, 0.008M and 0.01M) on the rGO-CS surface is analyzed. The diffraction peaks of silver nanoparticles from XRD analysis are in well accordance with the SAED pattern of HR-TEM. Moreover, the electrochemical property of the nanocomposites is studied using cyclic voltammetry.

The electrochemical sensing of p-Aminophenol at different pH of phosphate buffer solution and at different scan rate is also studied.

CHAPTER VI outlines the synthesis of rGO-CS nanocomposites and its decoration with various concentrations of gold nanoparticles (0.002 M, 0.004 M, 0.006 M, 0.008 M and 0.01 M) on its surface. The spherical shaped gold nanoparticles are well dispersed and closely anchored on the surface of rGO-CS nanosheets. The presence of functional group in the prepared samples is also studied by FTIR analysis. The diffraction peaks of gold nanoparticles from XRD analysis are in well accordance with the SAED pattern of HR-TEM. This chapter also describes the investigation of cyclic voltammetry studies for the detection of p-Aminophenol at different pH of phosphate buffer solution and at different scan rates.

CHAPTER VII describes the antibacterial and anticancer studies of the synthesized nanocomposites**.** The prepared nanocomposites are evaluated against gram-positive bacteria (Staphylococcus Aureus, Bacillus Subtilis) and gram-negative bacteria (Escherichia Coli, Klebsilla Pneumoniae) through disk diffusion method. The enhanced bactericidial activity is due to the generation of H_2O_2 molecules on the surface of prepared nanocomposites which can penetrate through the cell membrane and inhibit the growth of bacteria. The effect of anticancer is studied using the cytotoxicity effect. The cytotoxicity effect of the prepared nanocomposites is accomplished by MTT assay against liver cancer cell (HepG–2). The sample exhibits potential dose dependent cytotoxicity against HepG–2 (cancer cell line).

CHAPTER VIII concludes the summary of the results and conclusion.

REFERENCES

1. S. Logothetidis, Nanostructured Materials and Their Applications, NanoScience and Technology, DOI 10.1007/978-3-642-22227-6 1, (2012)
2. K. Eric. Drexler, Anchor Books and Doubleday, Engines of Creation :The Coming Era of Nanotechnology, (1986).
3. B. Bhushan, Springer Handbook of Nanotechnology, DOI 10.1007/978-3-319-49347-3_1, (2017)
4. Guozhong Cao, Nanostructures and Nanomaterials, Synthesis, Properties, and Applications, (2008)
5. Alain Nouailhat, ISBN: 978-1-84821-007-3
6. Physical Fundamentals of Nanomaterials, Elsevier, DOI: https://doi.org/10.1016/B978-0-12-410417-4.00008-3, (2018).
7. www.safenano.org
8. Satoshi Horikoshi and Nick Serpone, Introduction to Nanoparticles, (2013).
9. Jitendra N. Tiwari a, Rajanish N. Tiwari, Kwang S. Kim, Zero-dimensional, one-dimensional, two-dimensional and three-dimensional nanostructured materials for advanced electrochemical energy devices, Progress in Materials Science 57,724–803, (2012).
10. Jaison Jeevanandam , Ahmed Barhoum, Yen S. Chan, Alain Dufresne and Michael K. Danquah, Review on nanoparticles and nanostructured materials: history, sources, toxicity and regulations, Beilstein J. Nanotechnol, 9, 1050–1074, (2018).
11. Hassan Hassanien Mohamed Darweesh, Nanomaterials: Classification and Properties-Part I, Nanoscience, 1-11, (2017).

12. Dolez, P. I., Nanomaterials Definitions, Classifications, and Applications. Nanoengineering, 3–40, doi:10.1016/b978-0-444-62747-6.00001-4, (2015).

13. Sengupta, A and Sarkar, C. K, Introduction to Nano. Engineering Materials.doi:10.1007/978-3-662-47314-6, (2015)

14. Sandhiya sanand, Nanostructured materials; classification and methods of characterization, (2017).

15. www.docsity.com

16. Parvez Iqbal, Jon A. Preece and Paula M. Mendes, Nanotechnology: The "Top-Down" and "Bottom-Up" Approaches, DOI: 10.1002/9780470661 345.smc195, (2012)

17. Andres La Rosa, Mingdi Yan, Rodolfo Fernandez, Xiaohua Wang and Elia Zegarra, Top-down and Bottom-up approaches to nanotechnology

18. Dr. V.M.Arole and Prof.S.V.Munde, Fabrication of nanomaterials by top-down and bottom-up approaches – an overview , vol. 1,issue 2, page 89-93, (2014).

19. Gritsch L., Meng D and Boccaccini A. R, Nanostructured biocomposites for tissue engineering scaffolds. Biomedical Composites, 501–542, doi:10.1016/b978-0-08-100752-5.00021-4, (2017).

20. www.britannica.com

21. Salim Barbhuiya and i Curtin Uni, Applications of Nanotechnology in Cement and Concrete Science, DOI: 10.4018/978-1-4666-6363-3.ch029, (2014).

22. A S Edelstein and R C Cammarata, Nanomaterials: Synthesis, Properties and Applications

23. www.news-medical.net

24. Karak, N, Fundamentals of Nanomaterials and Polymer Nanocomposites. Nanomaterials and Polymer Nanocomposites, 1–45. doi:10.1016/b978-0-12-814615-6.00001-1, (2019). Op and elec

25. https://copublications.greenfacts.org/en/nanotechnologies/l-2/3-nanoparticle-properties.htm

26. Hong, N. H, Introduction to Nanomaterials: Basic Properties, Synthesis, and Characterization. Nano-Sized Multifunctional Materials, 1–19, doi:10.1016/b978-0-12-813934-9.00001-3, (2019).

27. www.shellzero.wordpress.com

28. Dan Guo, Guoxin Xie and Jianbin Luo, J, Mechanical properties of nanoparticles: basics and applications, Phys. D: Appl. Phys. 47, 013001, (2014)

29. Reghunadhan, A., Kalarikkal, N and Thomas, S, Mechanical Property Analysis of Nanomaterials. Characterization of Nanomaterials, 191–212, doi:10.1016/b978-0-08-101973-3.00007-9, (2018)

30. Taufeeque Hasan, Mechanical Properties of Nanomaterials: A Review, Vol-2 Issue-4 IJARIIE-ISSN(O)-2395-4396 , (2016)

31. Ibrahim Khan, Khalid Saeed , Idrees Khan, Nanoparticles: Properties, applications and toxicities, https://doi.org/10.1016/j.arabjc.2017.05.011, (2017)

32. Hoogeboom-Pot K, Hernandez-Charpak J, Frazer T, Gu X, Turgut E, Anderson, E. Nardi D, Mechanical and thermal properties of nanomaterials at sub-50nm dimensions characterized using coherent EUV beams. Metrology, Inspection, and Process Control for Microlithography XXIX.doi:10.1117/12.2085615, (2015).

33. Guozhong Cao, Ying Wang, Nanostructures and Nanomaterials: Synthesis, Properties, and Applications, (2011)

34. Zhypargul Abdullaeva, Nano and Biomaterials: Compounds, Properties, Characterization and Applications, (2017)

35. Mohan Bhagyaraj S and Oluwafemi O. SNanotechnology: The Science of the Invisible. Synthesis of Inorganic Nanomaterials, 1–18.doi:10.1016/b978-0-08-101975-7.00001-4, (2018).

36. https://winnerscience.com/2012/09/23/magnetic-properties-of-nanomaterials/

37. Mørup, S., Frandsen, C., & Hansen, M. F, Magnetic properties of nanoparticles. Oxford Handbooks, doi:10.1093/oxfordhb/9780199533053.013.20, (2017).

38. https://www.understandingnano.com/nanotech-applications.html

39. Nasrollahzadeh M, Sajadi S. M, Sajjadi, M and Issaabadi, Z, Applications of Nanotechnology in Daily Life, An Introduction to Green Nanotechnology, 113–143, doi:10.1016/b978-0-12-813586-0.00004-3, (2019).

40. Rakesh, Divya, Vishal and Shalini, J Nanomedine Biotherapeutic, Volume 5, Issue 1,1000131, DOI: 10.4172/2155-983X.1000131, (2015)

41. Ali Akbar Firoozi and Shariat Mobasser, Review of Nanotechnology Applications in Science and Engineering, J. Civil Eng. Urban, 6 (4),84-93, (2016)

42. Dr. Niranjani Chaurasia, Nanotechnology and Nanomaterials in Everyday Life, International Journal of Science and Research (IJSR) ISSN, 2319-7064, (2015)

43. Singh T, Shukla S, Kumar P, Wahla V, Bajpai, V. K and Rather, A. Application of Nanotechnology in Food Science: Perception and Overview. Frontiers in Microbiology, 8.doi:10.3389/fmicb.2017.01501, (2017).

44. Nasrollahzadeh M, Sajadi S. M, Sajjadi, M and Issaabadi, Applications of Nanotechnology in Daily Life. An Introduction to Green Nanotechnology, 113–143, doi:10.1016/b978-0-12-813586-0.00004-3, (2019).

45. Vijaya Shanti Bheemidi, Mrudula Tiruckovela, Naga Deepthi Chettipalli and Sree Venkateshwarlu Yanamadala, Novel Applications of Nanotechnology in Life Sciences, J Bioanal Biomed, doi:10.4172/1948-593X.S11-001, (2011)

46. Changjing Fu, Guogang Zhao, Haijun Zhang and Shuang Li, Evaluation and Characterization of Reduced Graphene Oxide Nanosheets as Anode Materials for Lithium-Ion Batteries, Int. J. Electrochem. Sci., 8, 6269 – 6280, (2013)

47. Indranil Roy., Dipak Rana., Gunjan Sarkar., Amartya Bhattacharyya., Nayan Ranjan Saha., Soumya Mondal., Sutanuka Pattanayak., Sanatan Chattopadhyay and Dipankar Chattopadhyay, RSC Advances, DOI: 10.1039/C4RA16197A, (2015)

48. N.I. Zaaba, K.L. Fooa, U. Hashim, S.J.Tan, Wei-Wen Liua and C.H. Voona, Synthesis of Graphene Oxide using Modified Hummers Method: Solvent Influence, Advances in Material & Processing Technologies Conference, Procedia Engineering 184, 469 – 477, (2017).

49. M. Nur Hossain, Jiali Wen and Aicheng Chen, Unique copper and reduced graphene oxide nanocomposite toward the efficient electrochemical reduction of carbon dioxide, Scientific reports, 7, 3184, DOI:10.1038/s41598-017-03601-3, (2017)

50. Z. Hu G. Tong, D. Lin, C. Chen, H. Guo Xu and L. Zhou, Graphene-reinforced metal matrix nanocomposites – a review, Materials Science and Technology, (2016)

51. Jonghoon Choi, Hana Oh, Sang-Wook Han, Seokhoon Ahn, Jaegeun Noh and Joon B. Park, Preparation and Characterization of Graphene Oxide Supported Cu, Cu2O, and CuO Nanocomposites and Their High Photocatalytic Activity for Organic Dye Molecule, S1567-1739(16)30335-2, (2016)

52. Zhimin Luo, Dongliang Yang, Guangqin Qi, Lihui Yuwen, Yuqian Zhang, Lixing Weng, Lianhui Wang and Wei Huang, Preparation of Highly Dispersed Reduced Graphene Oxide Decorated with Chitosan Oligosaccharide as Electrode Material for Enhancing the Direct Electron Transfer of Escherichia coli ACS Appl. Mater. Interfaces. 7, 8539−8544, (2015).

53. Zhihong Zhang, Xiaoming Fu, Kunzhen Li, Ruixue Liua, Donglai Peng, Linghao He ,Minghua Wang, Hongzhong Zhang and Liming Zhou, One-step fabrication of electrochemical biosensor based on DNA-modified three-dimensional reduced graphene oxide andchitosan nanocomposite for highly sensitive detection of Hg (II), Sensors and Actuators B 225, 453–462, (2016)

54. Arif D, Niazi M. B. K, Ul-Haq N, Anwar M. N and Hashmi E, Preparation of antibacterial cotton fabric using chitosan-silver nanoparticles. Fibers and Polymers, 16(7), 1519–1526, doi:10.1007/s12221-015-5245-6, (2015).

55. S. Archana, K.Yogesh Kumar,B.K. Jayanna, Sharon Olivera, A. Anand, M.K. Prashanth and H.B. Muralidhara, Versatile Graphene oxide decorated by star shaped Zinc oxide nanocomposites with superior adsorption capacity and antimicrobial activity, Journal of Science: Advanced Materials and Devices 3,167e174, (2018)

56. S. Gayathri., P. Jayabal., M. Kottaisamy and V. Ramakrishnan, Synthesis of ZnO decorated graphene nanocomposite for enhanced photocatalytic properties. Journal of Applied Physics, DOI: 10.1063/1.4874877, (2014).

57. Antonella Arena, Graziella Scandurra and Carmine Ciofi, Copper Oxide Chitosan Nanocomposite:Characterization and Application in Non-Enzymatic Hydrogen Peroxide Sensing, Sensors, 17, 2198; doi:10.3390/s17102198, (2017).

58. Sangiliyandi Gurunathan, Jae Woong, Han Jung Hyun, Park Eunsu Kim, Yun-Jung Choi Deug-Nam Kwon and Jin-Hoi Kim, Reduced graphene

oxide–silver nanoparticle nanocomposite: a potential anticancer nanotherapy, International Journal of Nanomedicine, (2015)

59. Sandhya P K, Jiya Jose, M S Sreekala, M Padmanabhana, Nandakumar Kalarikkal , Sabu Thomas, 2018, Reduced graphene oxide and ZnO decorated graphene for biomedical applications, Ceramics International , https://doi.org/10.1016/j.ceramint.2018.05.143.

60. Yan-Wen Wang, Aoneng Cao, Yu Jiang, Xin Zhang, Jia-Hui Liu, Yuanfang Liu, and Haifang Wang, Superior Antibacterial Activity of Zinc Oxide/Graphene Oxide Composites Originating from High Zinc Concentration Localized around Bacteria, doi;10.1021/am4053317.

61. Chandrama Sarkar and Swapan K. Dolui, Synthesis of copper oxide/reduced graphene oxide nanocomposite and its enhanced catalytic activity towards reduction of 4-nitrophenol, RSC Adv, 5, 60763–60769, (2015)

62. Kangfu Zhou, Yihua Zhu, Xiaoling Yanga, Jie Luo, Chunzhong Li and Shaorong Luan, A novel hydrogen peroxide biosensor based on Au–graphene–HRP–chitosan biocomposites, Electrochimica Acta, (2010).

63. Ajay Gupta, Ramen Jamatia, Ranjit A. Patil, Yuan-Ron Ma and Amarta Kumar Pal, Copper Oxide/Reduced Graphene Oxide Nanocomposite-Catalyzed Synthesis of Flavanones and Flavanones with Triazole Hybrid Molecules in One Pot: A Green and Sustainable Approach, ACS Omega, 3, 7288−7299, (2018).

64. J.Vinoth Kumar, R.Karthik, Shen-Ming Chen, K.Saravanakumar, Govindasamy Mani, V.Muthuraj, Novel hydrothermal synthesis of MoS_2 nanoclusters structure for sensitive electrochemical detection of human and environmental hazardous pollutant 4-aminophenol, RSC Advances, DOI: 10.1039/C6RA03343A, (2016).

65. Manish Kumar, Unni Krishnan, Pooja Devi and Akshay Kumar, Structural analysis of graphene oxide/silver nanocomposites optical properties,

electrochemical sensing and photocatalytic activity, J Mater Sci: Mater Electron, DOI 10.1007/s10854-017-7881-7, (2017).

66. Tama s Nemeth, Peter Jankovics, Ju lia Nemeth-Palota s, Hilda Ko, szegi-Szalai, Determination of paracetamol and its main impurity 4-aminophenol in analgesic preparations by micellar electrokinetic chromatography, Journal of Pharmaceutical and Biomedical Analysis, 47, 746–749, (2008).

67. Graziella Scandurra, Arena Antonella, Carmine Ciofi, Gaetano Saitta and Maurizio Lanza, Electrochemical Detection of p-Aminophenol by Flexible Devices Based on Multi-Wall Carbon Nanotubes Dispersed in Electrochemically Modified Nafion, Sensors, 14, 8926-8939; doi:10.3390/s140508926, (2014).

68. Priya Arulselvi Ramasubramanian, Sakthivel Thangavel, Gouthami Nallamuthu., Kiranpreethi Kirabakaran, Vinesh Vasudevan, Kennedy Ravichandran and Gunasekaran Venugopal, Journal of Materials Science: Materials in Electronics. https://doi.org/10.1007/s10854-018-8539-9, (2017).

69. Leandro Yoshio Shiroma, Murilo Santhiago, Angelo L. Gobbi, Lauro T. Kubota, Separation and electrochemical detection of paracetamol and 4-aminophenol in a paper-based microfluidic device, Electrochimica Acta, vol.194, pg.no:116–126, (2016).

70. Huanshun Yin, Qiang Ma, Yunlei Zhou, Shiyun Ai and Lusheng Zhu, Electrochemical behavior and voltammetric determination of 4-aminophenol based on graphene–chitosan composite film modified glassy carbon electrode, Electrochimica Acta 55,7,102–7108, (2010).

71. A.T.Ezhil Vilian,Vediyappan Veeramani, Shen-Ming Chen, Rajesh Madhu, Yun, Suk and Huh, Young-Kyu Han c, Preparation of a reduced graphene oxide/poly-lglutathione nanocomposite for electrochemical detection of 4-aminophenol in orange juice samples, Analytical methods, 00, 1-3, (2013).

72. Anna Regiel-Futyra, Ma gorzata Kus-Li kiewicz, Victor Sebastian, Silvia Irusta, Manuel Arruebo, Grazyna Stochel, and Agnieszka Kyzio, Development of non-cytotoxic chitosan-gold nanocomposites as efficient antibacterial materials, ACS Applied Materials & Interfaces, DOI: 10.1021/am508094e, (2014)

73. S. Govindan, E. A. K. Nivethaa, R. Saravanan, V. Narayanan and A. Stephen, (2012), Synthesis and characterization of chitosan–silver nanocomposite, Appl Nanosci 2:299–303.

74. Richard Justin and Biqiong Chen, Strong and conductive chitosan–reduced graphene oxide nanocomposites for transdermal drug delivery, J. Mater. Chem. B, 2, 3759–3770, (2014)

75. Dasan Mary Jaya Seema, Bullo Saifullah, Mariadoss Selvanayagam, Sivapragasam Gothai, Mohd Zobir Hussein, Suresh Kumar Subbiah, Norhaizan Mohd Esa and Palanisamy Arulselvan, Designing of the Anticancer Nanocomposite with Sustained Release Properties by Using Graphene Oxide Nanocarrier with Phenethyl Isothiocyanate

76. Yang L, Carbon nanostructures, Nanotechnology-Enhanced Orthopedic Materials, 97–120, doi:10.1016/b978-0-85709-844-3.00005-7, (2015).

77. http://theor.jinr.ru/disorder/carbon.html

78. Petr Slepicka, Tomas Hubacek, Zdenka Kolska, Simona Trostova, Nikola Slepickova Kasalkova, Lucie Bacakova and Vaclav Svorcík, The properties and applications of carbon nanostructure, Polymer science, (2010)

79. Chris Binns, Carbon Nanostructures: Bucky Balls and Nanotubes, Introduction to Nanoscience and Nanotechnology, (2010)

80. Nanocarbon, Fundamentals and Applications of Nano Silicon in Plasmonics and Fullerines, 287–309. doi:10.1016/b978-0-323-48057-4.00010-4, (2008).

81. Poole-Owens and Wolf, carbon nanostructures, Introduction to Nanoscience, Springer handbook, (2005)

82. T.C. Dinadayalane and J. Leszczynski, Fundamental Structural, Electronic, and Chemical Properties of Carbon Nanostructures: Graphene, Fullerenes, Carbon Nanotubes, and Their Derivatives, Handbook of Computational Chemistry,(2016)

83. Shenderova O. A, Zhirnov, V. V and Brenner D. W, Carbon Nanostructures. Critical Reviews in Solid State and Materials Sciences, 27(3-4), 227–356.doi:10.1080/1040843020850049, (2002).

84. Luis E. F. Foa Torres, Stephan Roche and Jean-Christophe Charlier, Introduction to Graphene-Based Nanomaterials: From Electronic Structure to Quantum Transport, Cambridge University Press, 978-1-107-03083-1, (2014)

85. Rafael Gregorio Mendes, Paweł S. Wróbel, Alicja Bachmatiuk, Jingyu Sun, Thomas Gemming, Zhongfan Liu and Mark Hermann Rümmeli, Carbon Nanostructures as a Multi-Functional Platform for Sensing Applications , Chemosensors, 6, 60, (2018)

86. C. Vacacela Gomez, E. Robalino, D. Haro, T. Tene, P. Escudero, A. Haro and J. Orbe, Structural and electronic properties of graphene oxide for different degree of oxidation, Materials Today: Proceedings 3,796 – 802, (2016)

87. https://www.ossila.com/pages/introduction-to-graphene

88. Jian Ru Gong, Graphene – Synthesis, Characterization, Properties and Applications, ISBN 978-953-307-292-0, (2011)

89. Spyrou K and Rudolf P, An Introduction to Graphene. Functionalization of Graphene,1–20, doi:10.1002/9783527672790, (2014).

90. Leila shahriary and anjali a. Athawale, Graphene oxide synthesized by using modified hummers approach, International Journal of Renewable Energy and Environmental Engineering, ISSN 2348-0157, Vol. 02, No. 01, (2014)

91. Challa Vijaya Kumar Ajith Pattammatte, Introduction to Graphene

92. John E. Proctor, Daniel Melendrez Armada and Aravind Vijayaraghavan, An Introduction to Graphene and Carbon Nanotubes, ISBN 9781498751797, (2017)

93. Jianguo Song, Xinzhi Wang and Chang-Tang Chang, Preparation and Characterization of Graphene Oxide, Journal of Nanomaterials, (2014)

94. Daniel R. Dreyer, Alexander D. Todd and Christopher W. Bielawski, Harnessing the chemistry of graphene oxide, Chem. Soc. Rev, (2014)

95. Shun Mao, Haihui Pu and Junhong Chen, Graphene oxide and its reduction: modeling and experimental progress, RSC Advances, 2, 2643–2662, (2012)

96. Sen, Nainar and Begum, Model, synthesis and applications of graphene oxide: a review, (2014)

97. Dreyer D. R.,Park, S, Bielawski, C. W and Ruoff, R. S, The chemistry of graphene oxide, Chem. Soc. Rev, 39(1), 228–240, doi:10.1039/b917103g, (2010).

98. Klaus Muellen and Xinliang Feng, Chemistry of Carbon Nanostructures, (2017)

99. Sun Ling and Beijing Guyue, Structure and Synthesis of graphene oxide, New Materials Research Institute, College of Material Science & Engineering, Beijing University of Technology Pingleyuan

100. Jun Zeng, Rui-Qin Zhang and Herbert Treutlein, Quantum Simulations of Materials and Biological Systems, (2012)

101. https://www.understandingnano.com/graphene-properties.html

102. https://www.graphene-info.com/graphene-properties.

103. https://www.cheaptubes.com/graphene-synthesis-properties-and-applications/

104. Dimitrios G. Papageorgiou, Ian A. Kinloch, Robert J. Young, Mechanical properties of graphene and graphene-based nanocomposites, Progress in Materials Science 90, 75–127, (2017)

105. R. Vajtai, Aravind Vijayaraghavan, Springer Handbook of Nanomaterials, DOI 10.1007/978-3-642-20595-8_2, (2013)

106. https://www.nanowerk.com/what_is_graphene.php

107. Dispersion of Graphene in the Polymer Matrix (rgo)

108. Mohsen Moazzami Gudarzi, Seyed Hamed Aboutalebi and Farhad Sharif, Graphene Oxide based Composite Materials

109. Yu Chen, Bin Zhang, Gang Liu, Xiaodong Zhuang and En-Tang Kang, Graphene and its derivatives: switching ON and OFF, Chem. Soc. Rev, 41, 4688–4707, (2012)

110. Anahita Karimi, Ali Othman, Aytekin Uzunoglu, Lia Stanciub and Silvana Andreescu, Graphene based enzymatic bioelectrodes and biofuel cells, Nanoscale, 7, 6909, (2015)

111. Tapas Kuil, Saswata Bose, Ananta Kumar Mishra, Partha Khanra, Nam Hoon Kim and Joong Hee Lee, Chemical functionalization of graphene and its applications, Progress in Materials Science 57, 1061–1105, (2012)

112. Horacio J. Salavagione, Gerardo Martínez and Gary Ellis, Graphene-Based Polymer Nanocomposites, Institute of Polymer Science and Technology, Spanish National Research Council (CSIC) Spain

113. Andrew T. Smith, Anna Marie LaChance, Songshan Zeng, Bin Liu and Luyi Sun, Synthesis, properties and applications of graphene oxide/reduced graphene oxide and their nanocomposites

114. Krzysztof Tadyszak, Jacek K. Wychowaniec and Jagoda Litowczenko, Biomedical Applications of Graphene-Based Structures, Nanomaterials, 8, 944; doi:10.3390/nano8110944, (2018)

115. Madhab Bera and Pradip K Maji, Graphene-based polymer nanocomposites: materials for future revolution, MOJ Poly Sci, 2017,1(3), 94–97, (2017)

116. Polymer-Graphene Nanocomposites: Preparation, Characterization, Properties, and Applications http://dx.doi.org/10.5772/50408

117. Lizardi-Mendoza J, Argüelles Monal W. M and Goycoolea Valencia, F. M. Chemical Characteristics and Functional Properties of Chitosan. Chitosan in the Preservation of Agricultural Commodities, 3–31.doi:10.1016/b978-0-12-802735-6.00001-x, (2016).

118. Duarte Moura, João F. Mano, Maria C. Paiva and Natália M. Alves, Chitosan nanocomposites based on distinct inorganic fillers for biomedical applications, Sci. Technol. Adv. Mater. 17, 627, (2016).

119. Daniel Elieh-Ali-Komi and Michael R Hamblin, Chitin and Chitosan: Production and Application of Versatile Biomedical Nanomaterials

120. Majeti N.V. Ravi Kumar, A review of chitin and chitosan applications, Reactive & Functional Polymers, 46, 1–27, (2000)

121. Daniel Elieh-Ali-Komi and Michael R Hamblin, Chitin and Chitosan: Production and Application of Versatile Biomedical Nanomaterials, Int J Adv Res, 4(3), 411–427, (2016)

122. Santhana Krishna Kumara and Shiuh-Jen Jiang, Chitosan-functionalized graphene oxide: A novel adsorbent an efficient adsorption of arsenic from aqueous solution, S2213-3437(16)30079, (2016).

123. Sánchez-Machado D. I, López-Cervantes J, Correa-Murrieta M. A, Sánchez-Duarte, R. G, Cruz-Flores and de la Mora-López G. S, Chitosan. Nonvitamin and Nonmineral Nutritional Supplements, 485–493.doi:10.1016/b978-0-12-812491-8.00064-3, (2019)

124. Li Q, Dunn E. T, Grandmaison E. W and Goosen, M. F. A. Applications and Properties of Chitosan. Journal of Bioactive and Compatible Polymers, 7(4), 370–397, doi:10.1177/088391159200700406 (1992).

125. Elson Santiago de Alvarenga, Characterization and Properties of Chitosan, Biotechnology of Biopolymer, (2011)

126. Mody V, Siwale, R, Singh A and Mody H, Introduction to metallic nanoparticles. Journal of Pharmacy and Bioallied Sciences, 2(4), 282. doi:10.4103/0975-7406.72127, (2010).

127. Fatemeh Parnianchi, Maryam Nazari, Jila Maleki and Marjan Mohebi, Combination of graphene and graphene oxide with metal and metal oxide nanoparticles in fabrication of electrochemical enzymatic biosensors, International Nano Letters, 8, 229–239, (2018)

128. T Yao, Encyclopedia of Materials: Science and Technology, ISBN: 0-08-0431526, (2001)

129. Agnieszka Kołodziejczak-Radzimska and Teofil Jesionowski, Zinc Oxide—From Synthesis to Application: A Review, Materials, 7, 2833-2881; doi:10.3390/ma7042833, (2014)

130. Umit Ozgu r, Vitaliy Avrutin and Hadis Morkoc, Zinc Oxide Materials and Devices Grown by Molecular Beam Epitaxy Molecular Beam Epitaxy, Springer, (2018)

131. Zhong Lin Wang J, Zinc oxide nanostructures: growth, properties and applications, Phys.: Condens. Matter 16, R829–R858, (2004)

132. Desai A. V and Haque M. A, Mechanical properties of ZnO nanowires. Sensors and Actuators A: Physical, 134(1), 169–176.doi:10.1016/ j.sna.2006.04.046, (2007).

133. Vandana Parihar, Mohan Raja And Rini Paulose, A Brief Review of Structural, Electrical And Electrochemical Properties of Zinc Oxide Nanoparticles, Rev.Adv.Mater.Sci, 53, 112-130, (2018)

134. https://en.wikipedia.org/wiki/Copper(II)_oxide

135. Lanje,Satish J. Sharma, Ramchandara B. Pode, Raghumani S. Ningthoujam, Synthesis and optical characterization of copper oxide nanoparticles Amrut. S. Advances in Applied Science Research, 2010, 1 (2): 36-40

136. Tiginyanu I. M, Lupan O, Ursaki V. V, Chow, L and Enachi, M. Nanostructures of Metal Oxides. Comprehensive Semiconductor Science and Technology, 396–479.doi:10.1016/b978-0-44-453153-7.00105-x, (2011).

137. Robert Patrick Allaker, Nanoparticles and the Control of Oral Biofilms

138. Madalina Elena Grigore, Elena Ramona Biscu, Alina Maria Holban Monica Cartelle Gestal and Alexandru Mihai Grumezescu, Methods of Synthesis, Properties and Biomedical Applications of CuO Nanoparticles.

139. Jun Natsuki, Toshiaki Natsuki and Yoshio Hashimoto, A Review of Silver Nanoparticles: Synthesis Methods, Properties and Applications, International Journal of Materials Science and Applications, 4(5), 325-332, (2015)

140. https://www.purestcolloids.com/silver-atom-structure.php

141. http://weppi.gtk.fi/publ/foregsatlas/text/Ag.pdf

142. https://www.lenntech.com/periodic/elements/ag.htm

143. https://www.azonano.com/article.aspx?ArticleID=3284

144. Schroffenegger M and Reimhult E, Thermoresponsive Core-Shell Nanoparticles and their potential applications, Reference Module in Materials Science and Materials Engineering, doi:10.1016/b978-0-12-803581-8.10431-x, (2018).

145. https://www.chem.uci.edu/~dmitryf/manuals/Fundamentals/FTIR%20principles.pdf

146. Markovich R. J and Pidgeon C, Pharmaceutical Research, 08(6), 663–675, doi:10.1023/a:1015829412658, (1991)

147. Hideo Toyara, Introduction to XRD analysis using diffraction method, Rigaku Journal, 32(2), 35-43, (2016)

148. S T Misture and R L Snyder, X-ray Diffraction, Encyclopedia of Materials: Science and Technology, 9799–9808, doi:10.1016/b0-08-043152-6/01778-2, (2001).

149. Andres Kaech, An Introduction to Electron Microscopy Instrumentation, Imaging and Preparation, Center for Microscopy and Image Analysis, University of Zurich

150. Brandon Cheney, Introduction to Scanning Electron Microscopy

151. James A. Seyforth, Scanning Electron Microscopy (SEM): An Introduction to the use of SEM for characterising the Surface Topology and Composition of Matter with Further Applications, Experimental Techniques In Condensed Matter Physics, (2016).

152. https://www.fei.com/introduction-to-electron-microscopy/tem/

153. Goodhew P, General Introduction to Transmission Electron Microscopy (TEM). Aberration-Corrected Analytical Transmission Electron Microscopy, 1–19, doi:10.1002/9781119978848.ch1, (2011)

154. http://www.ammrf.org.au/myscope/pdfs/tem.pdf

155. Wang Wen, Introductory Chapter: What is Chemical Sensor, DOI: 10.5772/64626, (2016)

156. https://www.engineersgarage.com/article_page/sensors-different-types-of-sensors/

157. Aoife C. Power and Aoife Morrin, Electroanalytical Sensor Technology, http://dx.doi.org/10.5772/51480, (2013)

158. http://www.chem.ucla.edu/~bacher/CHEM174/equipment/CV1.html

159. Russian Journal of Electrochemistry, 38(12), 1364–1365, doi:10.1023/ a:1021637209564, (2002).

160. https://en.wikipedia.org/wiki/Auxiliary_electrode

161. Kahlert H, Reference Electrodes. Electroanalytical Methods, 261–278, doi:10.1007/978-3-662-04757-6_14, (2005)

162. Noemie Elgrishi, Kelley J. Rountree, Brian D. McCarthy, Eric S. Rountree, Thomas T. Eisenhart and Jillian L. Dempsey, A Practical Beginner's Guide to Cyclic Voltammetry

163. Peter T. Kissinger and William R. Heineman, Journal of Chemical Education, 702-706

164. Joshi P.S.and Sutrave, A Brief Study of Cyclic Voltammetry and Electrochemical Analysis D.S International Journal of ChemTech Research CODEN (USA): IJCRGG, ISSN: 0974-4290, ISSN-2455-9555, Vol.11 No.09, pp 77-88, (2018)